Construction of multivalent homo- and hetero-functional ABO blood group glycoconjugates using a trifunctional linker strategy

Gour Chand Daskhan[1], Hanh-Thuc Tran[1], Peter J. Meloncelli[1], Todd L. Lowary[1,3], Lori J. West[1,2,3] and Christopher W. Cairo[1,3]*

[1]Alberta Glycomics Centre, Department of Chemistry, University of Alberta, Edmonton Alberta, T6G 2G2, Canada

[2]Department of Pediatrics, Surgery, Medical Microbiology/Immunology and Laboratory Medicine/Pathology; Alberta Transplant Institute, University of Alberta Edmonton, AB, T6G 2E1

[3]Canadian National Transplant Research Program, University of Alberta, Edmonton, AB, T6G 2E1

*To whom correspondence should be addressed. Tel.: 780 492 0377; fax: 780 492 8231; e-mail: ccairo@ualberta.ca

ABSTRACT

The design and synthesis of multivalent ligands displaying complex oligosaccharides is necessary for the development of therapeutics, diagnostics, and research tools. Here, we report an efficient conjugation strategy to prepare complex glycoconjugates with four copies of one or two separate glycan epitopes, providing 4–8 carbohydrate residues on a tetravalent poly(ethylene glycol) scaffold. This strategy provides complex glycoconjugates that approach the size of glycoproteins (15–18 kDa) while remaining well-defined. The synthetic strategy makes use of three orthogonal functional groups, including a reactive NHS-ester moiety on the linker to install the first carbohydrate epitope via reaction with an amine. A masked amine functionality on the linker is revealed after removal of a fluorenylmethyloxycarbonyl (Fmoc)-protecting group, allowing attachment to the NHS-activated PEG scaffold. An azide group in the linker was then used to incorporate the second carbohydrate epitope via catalyzed alkyne–azide cycloaddition. Using a known tetravalent PEG-scaffold (PDI, 1.025), we prepared homofunctional glycoconjugates that display four copies of lactose, the A-type II or the B-type II human blood group antigens. Using our trifunctional linker, we expanded this strategy to produce heterofunctional conjugates with four copies of two separate glycan epitopes. These heterofunctional conjugates included Neu5Ac, or 3'-sialyllactose, or 6'-sialyllactose as a second antigen. Using an alternative strategy, we generated heterofunctional conjugates with three copies of the glycan epitope and one fluorescent group (on average) using a sequential dual-amine coupling strategy. These conjugation strategies should be easily generalized for conjugation of other complex glycans. We demonstrate that the glycan epitopes of heterofunctional conjugates engage and cluster target BCR and CD22 receptors on B cells, supporting the application of these reagents for investigating cellular response to carbohydrate antigens of the ABO blood group system.

INTRODUCTION

Glycoconjugates, including glycoproteins, serve important roles in biological systems. Glycans can impart stability, provide specificity, alter protein conformation, and provide numerous structural functions.[1] A common feature of glycoconjugates is their heterogeneity due to the non-template driven biosynthetic processes involved in their generation.[2] As a result, glycobiology as a field must develop tools for structural determination in addition to developing reliable methods for purification and synthesis of homogenous glycoconjugates.[3-6] Many biologically active glycoconjugates are of high molecular weight, and may display glycans that are larger than the scaffold to which they are attached.[7-9] Another common feature of naturally occurring glycoconjugates is the presence of multiple glycan epitopes. Thus, an ongoing challenge in glycobiology is to establish methods that allow the attachment of glycans to large scaffolds, with precise control of copy number for one or more glycan epitopes.

Synthetic multivalent glycoconjugates are widely used as tools for glycobiology and biomedical applications.[10-12] Over the last decade, many examples of homo- and heterofunctional glycoconjugates have been synthesized using core scaffolds including sugars,[13,14] peptides,[15,16] dendrimers,[17] cyclodextrins,[18] polymers,[19] quantum dots,[20] nanoparticles,[21, 22] and cyclopeptides.[23] The manner in which glycans are presented on different scaffolds can be important for specific applications.[24, 25] Most strategies to construct multivalent glycoconjugates take advantage of the expanding palette of biorthogonal coupling reactions[26, 27] including thiol–ene coupling (TEC),[28] copper (I)-catalyzed alkyne–azide cycloaddition (CuAAC),[29] thiol–chloroacetyl coupling,[30,31] oxime ligation,[32] or combinations of these with amide coupling or disulphide bond formation.[22, 33]

The presentation of glycoconjugates in biological systems is often multivalent, thus synthetic strategies that mimic this display are often critical for applications. Glycans and glycoconjugates can act as important antigens for the development of adaptive immunity.[34] Synthetic glycoconjugates are used in vaccines to mimic the presentation of glycans from pathogens and elicit the production of antibodies.[35] Glycans are also important recognition factors in regulation of the immune response, where they may act on lectin receptors to modulate cellular immunity.[36]

B cells are a critical component of cellular immunity and autoimmune disease, and rely on specific molecular cues for their regulation.[37] Recognition and binding of specific antigens to the B cell receptor (BCR) complex results in B cell activation, proliferation, and antibody production.[38] Recognition of α-(2→3) and α-(2→6)-linked sialic acids by Siglec-G and CD22 co-receptors are known to attenuate B cell activation,[39] and are important for the development of immune tolerance.[40-44] Indeed, colocalization of BCR and CD22 leads to B cell deactivation.[45] Glycoconjugates that simultaneously display a BCR antigen (2,4-dinitrophenyl, DNP) and an α-(2→6) linked sialyllactose (as a CD22 ligand) induce B cell tolerance by interacting with both receptors.[46-50] There have been several examples of multivalent homogeneous[51,52] and bifunctional[43, 46-49, 53] ligands designed to promote B cell tolerance. These studies have raised the possibility of designing glycoconjugates as tolerance-inducing molecules, termed *tolerogens*.[54-56] However, it remains to be investigated whether more diverse antigens, such as carbohydrate antigens, can induce B cell tolerance through co-presentation of Siglec ligands. Our groups have been interested in understanding the development of antibodies to the ABO human blood group antigens (HBGA). Elimination of

anti-ABO antibodies in both organ and bone marrow transplantation would expand the safe use of blood products.[57, 58]

The human ABO blood group system was first described by Karl Landsteiner in the early 20th century.[59,60] The ABO system is characterized by expression of ABH carbohydrate structures on human erythrocytes and other tissues generally derived from embryonic mesoderm. ABO-incompatibility is a major challenge for blood transfusion and organ transplantation due to pathologic effects of 'natural' antibodies to non-self A/B antigens that are produced as a presumed immunologic cross-reaction to similar epitopes from the gut microbiome. An exception has been demonstrated in young children, who can safely receive ABO-incompatible heart transplants due to their normal developmental lag in production of anti-ABO antibodies.[61] Spontaneous development of immune tolerance to donor blood group A and B antigens has been observed after ABO-incompatible heart transplantation in children with immature immune systems.[58, 62] We recently characterized the expression of ABH subtype structures in heart tissue,[63] and using a novel ABH glycan microarray to probe patient sera, demonstrated the fine specificity of donor-specific B cell tolerance in this setting.[64] Recognition and detection of A/B-specific B cell populations using ABH carbohydrate antigens is also important for clinical applications in transfusion medicine and organ transplantation as well as studying mechanisms of ABO tolerance. We have also investigated the use of fluorescently-labelled silica microparticles functionalized with A and B blood group structures for detection of A and B antigen-reactive B cells by flow cytometry and fluorescence microscopy.[22]

We considered that a tolerogen displaying both an A and/or B antigen together with a Siglec ligand could be effective for tolerance induction in advance of transplantation, allowing a strategy for safe use of ABO-incompatible organs beyond infancy. B cell tolerance

to ABH antigens has been induced by using very high concentrations of the blood group antigens in baboon.[65] Conjugates used to induce tolerance in B cells have included linear polymers, branched PEG, and liposome scaffolds.[46-49, 66-69]Any tolerogen design must allow for control of the relative stoichiometries of the BCR-antigen and Siglec-ligand interactions. A variety of strategies have been explored for attachment of carbohydrate antigens to scaffolds including the use of squarates,[70-74] di-*p*-nitrophenyl adipate,[75-79] di-*N*-succinimidyl adipate,[80, 81] CuAAC ligation,[82] maleimides,[83,84] and NHS-activated esters.[85] The design of a conjugation strategy for ABO tolerogens must be versatile enough to allow easy modification of each component, and should ideally allow for introduction of fluorescent tags or other handles.

Herein, we describe a conjugation method based on amine coupling alone or in combination with CuAAC and a heterotrifunctional linker. This method produces well-defined multivalent homo- and hetero-bifunctional scaffolds containing synthetic carbohydrate antigens and Siglec ligands. The scaffolds are based on a commercially available tetravalent poly(ethylene glycol) (PEG) platform, which has been previously explored for the display of peptide antigens.[67,68] Similar PEG scaffolds have found many applications in biochemistry and drug delivery because of their prolonged *in vivo* circulation half-lives, water solubility, flexibility, low polydispersity, and low immunogenicity.[86-89] We generated a series of ligands with variation in the carbohydrate antigens, including lactose, the A-type II HBGA, and the B-type II HBGA. These antigens were efficiently conjugated with NHS-activated PEG scaffolds via an amine to afford defined tetravalent homogenous glycoconjugates. In addition, the synthesis of AlexaFluor-labelled lactose and A-type II conjugates was performed through iterative amine coupling. To generate heterobifunctional sialoglycoconjugates, we developed a heterotrifunctional linker compatible with amine-

containing antigens. A second co-receptor ligand was installed via CuAAC ligation. This strategy enabled us to generate a panel of structurally well-defined multivalent homogenous glycoconjugates of high molecular weight (12–18 kDa), which could be modified to feature fluorescent labels and sialoglycosides. Finally, we explored the biological activity of these compounds using a B cell line with A-type II-specific BCR to confirm that these compounds effectively cluster and co-localize BCR and CD22 on live cells.

RESULTS AND DISCUSSION

Synthesis of amine terminated carbohydrate antigens. The carbohydrate antigens **1**, **3**, and **4** (Scheme 1) bearing an alkene moiety were prepared as previously reported.[90] These antigens were functionalized with an amine by employing UV-promoted (λ = 254 nm) TEC.[91] Photoinduced radical addition of the cysteamine hydrochloride salt (10 equiv) to octenyl lactoside (**1**) was conducted in anhydrous MeOH for 45 min under an argon atmosphere.[92] The product was purified by C-18 chromatography followed by treatment with Dowex resin (HO^-) to provide free amine **2** (88% yield). Synthesis of the amine-terminated tetrasaccharide A-type II (**5**) and B-type II (**6**) were achieved starting from known intermediates **3** and **4** in good yields following a similar TEC protocol.

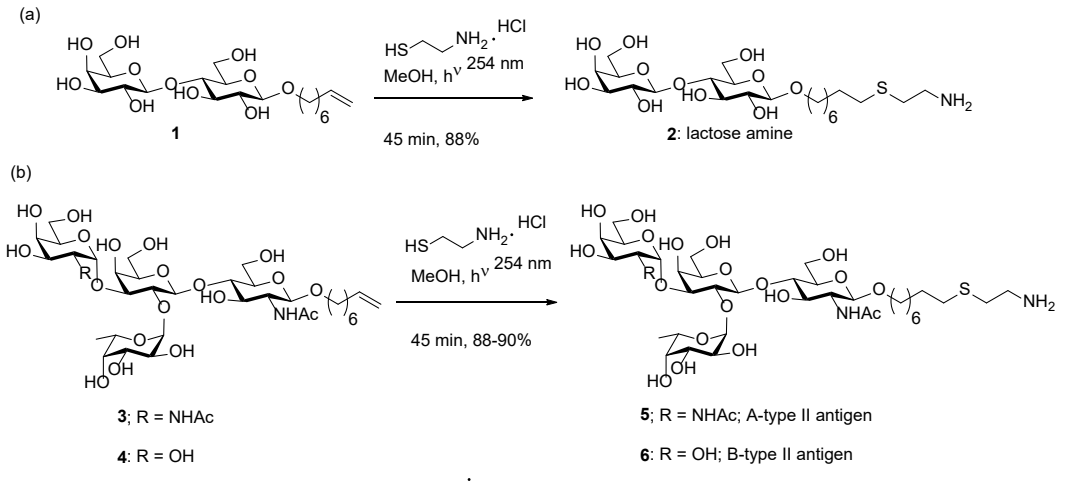

Scheme 1. Synthesis of the amine-terminated carbohydrate antigens

Synthesis of tetravalent homofunctional glycoconjugates. The synthesis of homofunctional tetravalent glycoconjugates (compound **8–10** and **12–14**, Scheme 2) was achieved through the amine coupling of carbohydrate antigens with commercially available tetravalent NHS-activated PEG scaffolds (**7** and **11**, 11.2 kDa). After optimizing reaction conditions, we found that the coupling between the carbohydrate amine (1.25 equiv per NHS-ester) and the NHS-activated PEG scaffold proceeded in good yields under anhydrous conditions in the presence of base (*N,N*-diisopropylethylamine, DIPEA). Thus, carbohydrate antigens **2**, **5**, and **6** were efficiently conjugated with scaffold **7** (11.2 kDa) to afford tetravalent conjugates **8** (12.8 kDa), **9** (14.4 kDa), and **10** (14.2 kDa) in 90–94% yields (Scheme 2). The progress of the coupling was monitored by TLC using ninhydrin staining to observe consumption of the carbohydrate amine. After ~24 h, the crude product was purified by C-18 chromatography. The tetravalent structures were characterized by analysis of the ^{1}H and ^{13}C NMR and MALDI-TOF-MS spectroscopies (see general methods in Experimental Procedures). No traces of the incompletely reacted side products were detected.

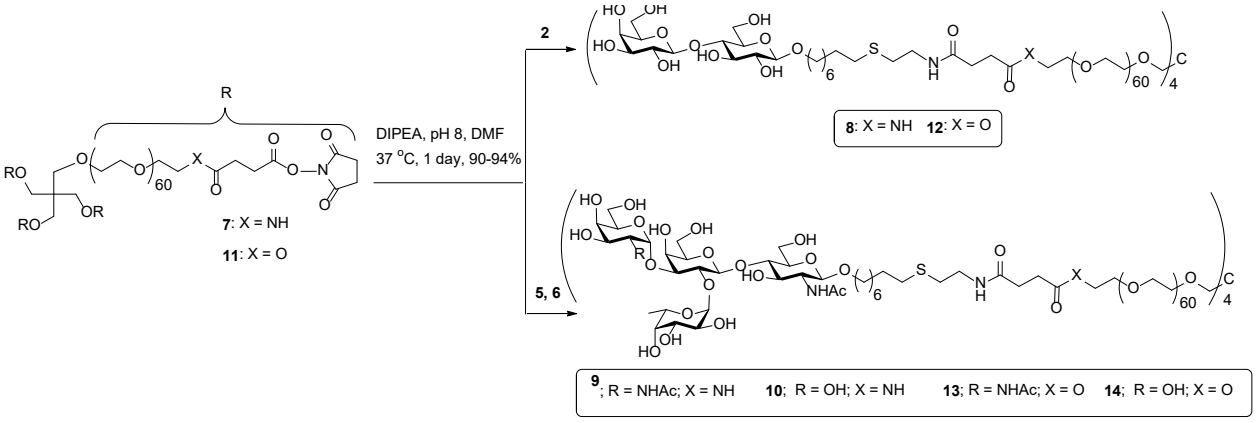

Scheme 2. Synthesis of homogenous tetravalent glycoconjugates

A PEG scaffold with an ester linkage, **11** (11.2 kDa), was also conjugated with amines **2**, **5**, and **6** using identical coupling conditions as those used for **7**. The ester linkage is expected to be less stable in serum and could provide a useful comparison of the role of conjugate stability *in vivo*. After purification, tetravalent structures **12** (12.8 kDa), **13** (14.4 kDa), and **14** (14.2 kDa), were generated in quantitative yields. The degree of substitution was determined by analysis of the ^{1}H NMR spectrum of conjugate **12** using integration of the anomeric H-1 and H-1' signals at 4.43 ppm (J = 7.8 Hz) and 4.40 ppm (J = 7.8 Hz), together with the PEG-COCH_2CH_2CO- observed at 2.49 ppm (broad singlet). A comparison of MALDI-TOF mass spectroscopic data (Figure 1C) showed an increase of average molecular mass of 1.6 kDa (calculated 1.6 kDa) for conjugate **12** (12.8 kDa) with respect to NHS-activated PEG **11** (11.2 kDa). The PEG repeating unit (44 Da) is visible in the mass spectra, and the observed shift of mass along with the ^{1}H NMR integrations confirmed the synthesis of the desired conjugate.

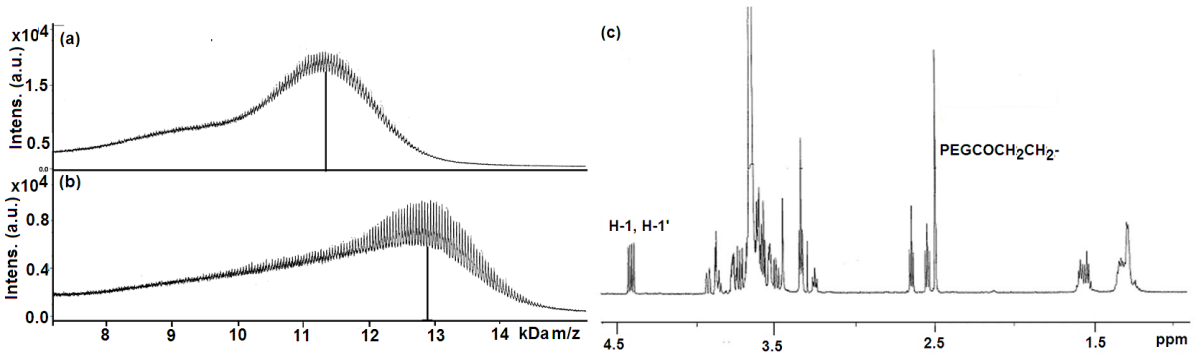

Figure 1. (a) MALDI-TOF-MS profile of NHS-activated PEG **11** (Avg mol. wt. 11.2 kDa) and (b) conjugate **12** (Avg mol. wt. 12.8 kDa; lactose:PEG = 4:1) and black line indicates centre of mass, and (c) anomeric H'-1, H-1 and PEG-COCH_2CH_2CO- at 4.43, 4.40, and 2.49 ppm in the ^{1}H NMR (600 MHz, D_2O) spectrum of conjugate **12**.

Synthesis of AlexaFluor-labeled glycoconjugates. The development of a highly efficient conjugation strategy for the labeling of biomolecules is essential for the quantitative analyses of their role in cell biology. We implemented an iterative amine coupling strategy to synthesize well-defined multivalent fluorescent-labeled glycoconjugates in a controlled and stoichiometric-dependent fashion. We selected AlexaFluor 488 (λ_{ex} = 493 nm, λ_{em} = 516 nm) because it is pH-stable, photostable, and bright, making it practical for live-cell fluorescent imaging.[93] The fluorescent dye-bearing amine was coupled first, followed by addition of the carbohydrate amine with the NHS-activated PEG scaffold (11.2 kDa). The average level of incorporation of the fluorescent dye and carbohydrate structure to the PEG scaffold was calculated by comparison of the aromatic protons of the fluorescent moiety and anomeric protons of the carbohydrate structure in the ^{1}H NMR spectrum. Two AlexaFluor-labeled conjugates (**16** and **17**) were synthesized at a substitution ratio (dye to carbohydrate) of 1.3:2.7 and 0.6:3.4 based on ^{1}H NMR spectroscopy, in 90% and 91% respective yields (Scheme 3). To prepare conjugate **16** (12.9 kDa), amine **15** was reacted with **7** in the presence of DIPEA in anhydrous DMF at room temperature. Subsequently, a second amine coupling incorporated the lactose amine **2** (1.65 mg, 3.12 μmol, 3.5 equiv) into the unreacted NHS-activated PEG adduct followed by an additional ~21 h incubation under identical conditions. MALDI-TOF mass spectroscopic data showed an increase of average molecular mass of 1.4 kDa (calculated 1.8 kDa) for conjugate **16** (13.0 kDa) with respect to NHS-activated PEG **11** (11.2 kDa). With a strategy for controlling the stoichiometry of two amines established, generated a fluorescent-tagged A-type II-conjugate **17** (14.0 kDa) from **15, 7**, and antigen **6** following a similar protocol.

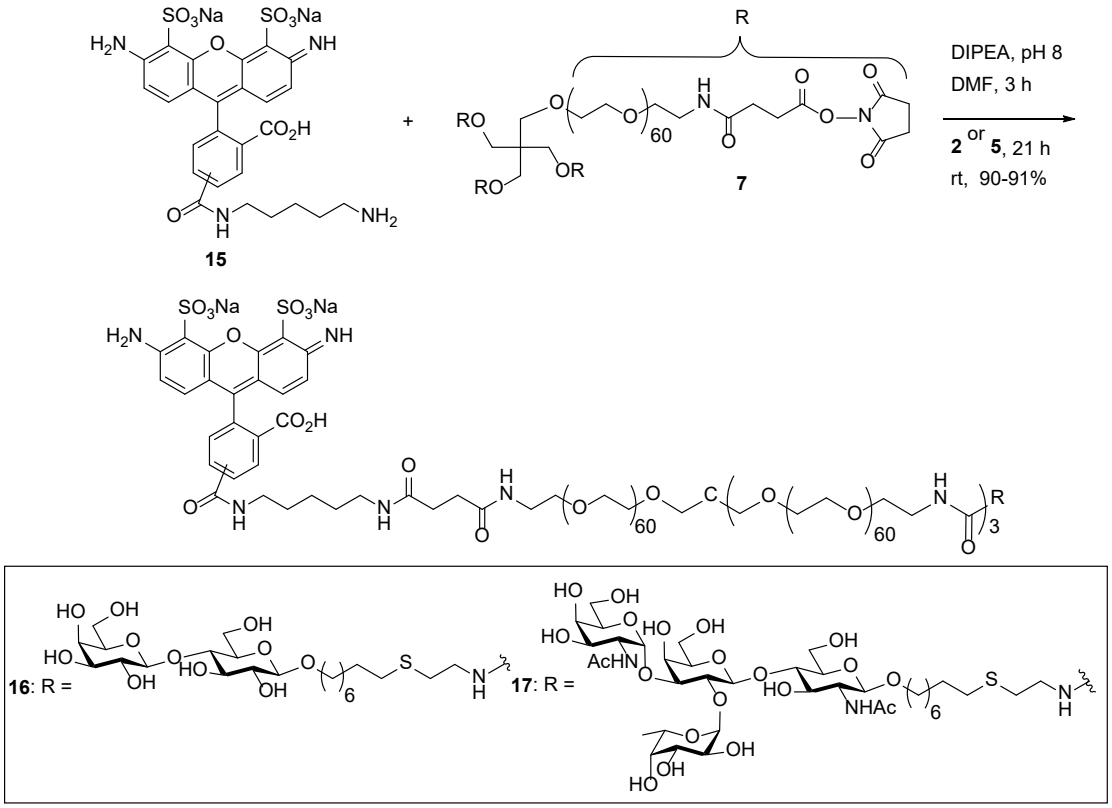

Scheme 3. Synthesis of AlexaFluor-labeled glycoconjugates **16** (AlexaFlour:lactose:PEG = 1.3:2.7:1) and **17** (AlexaFlour:A-type II:PEG = 0.6:3.4:1) using iterative amine coupling

Design and synthesis of a heterotrifunctional linker. To generate heterofunctionalized conjugates, a suitable linker had to be identified based on solubility, reactivity, coupling efficiency, stability, and ease of purification. To this end, we developed a novel heterotrifunctional linker (**21**, Scheme 4) terminated with three functional groups: a reactive NHS-ester, an Fmoc-protected amine, and an azide. The orthogonal reactivity of this linker was designed to be compatible with the conjugation strategies outlined above. The NHS-ester of **21** would first be reacted with the amine of an antigen. This would be followed by removal of the Fmoc-protecting group, and coupling to the NHS-ester of the PEG scaffold. The

resulting azide-containing product would then be reacted with propargyl-containing antigens via CuAAC to generate the final conjugate.

The heterotrifunctional linker **21** was synthesized using a solid-phase synthetic strategy from Fmoc-Lys-OH, which was converted to Fmoc-Lys(N_3)-OH (**18**) using imidazole-1-sulphonyl azide as the diazotransfer reagent.[94, 95] Once its preparation was complete, **18** was coupled to 2-chlorotrityl chloride resin in the presence of DIPEA in CH_2Cl_2. Subsequent treatment with commercial Fmoc-9-amino-4,7-dioxanonanoic acid (**19**)[96] using HBTU[97] activation provided the resin-bound derivative of compound **20**. Cleavage from the resin with trifluoroacetic acid afforded **20** in quantitative yield after purification by silica gel chromatography. For conjugation to amines, **20** was converted to its *N*-hydroxysuccinimidyl ester via reaction with NHS and dicyclohexylcarbodiimide (DCC) in CH_2Cl_2 to afford **21** in 86% yield after purification (Scheme 4).

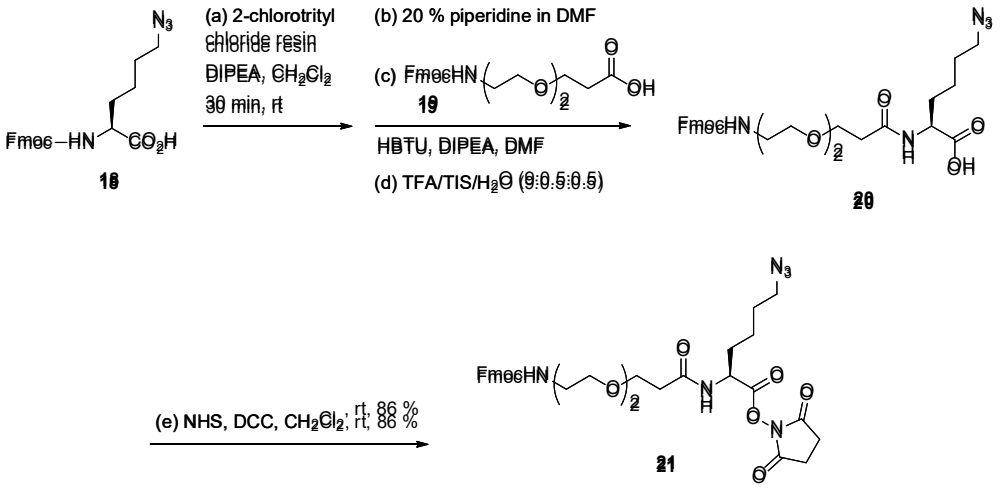

Scheme 4. Solid-phase synthesis of heterotrifunctional linker **21**

Synthesis of an octavalent heterobifunctional glycoconjugate. With linker **21** in hand, we turned our attention to the synthesis of heterobifunctional sialoglycoconjugates. We sought to

develop an efficient conjugation protocol using sequential dual amine coupling in combination with CuAAC ligation. To demonstrate this conjugation strategy, we made a series of octavalent sialoglycoconjugates (Scheme 5). The lactose amine **2** was coupled with the NHS-ester of **21** in the presence of DIPEA in anhydrous DMF at room temperature for 6 h. Subsequently, the Fmoc-protecting group on the linker was removed with 20% piperidine in DMF at room temperature for 1 h. This one-pot, two-step reaction afforded **22** in a 74% yield after semi-preparative RP-HPLC purification. In the second step, the free amine of **22** (1.25 equiv per NHS-ester) was subjected to a second coupling with NHS-activated PEG scaffold **7** (11.2 kDa) as above. The reaction mixture was incubated at room temperature for 3 h, and an additional 21 h at 37 °C. Upon completion of the reaction, as determined by TLC, the crude product was purified using C-18 chromatography to afford lactose conjugate **23** in 94% yield as a colorless powder after lyophilization. The tetravalent structure of conjugate **23** (14.1 kDa), displayed four copies of the azide group as established by ^{1}H NMR spectroscopy. Analysis by MALDI-TOF MS showed a loss of azide groups and the fragmentation of carbohydrate (see Experimental Procedures). However, this appears to be an artifact of MS as the azide was found to be intact in later steps (vide infra).

The A-type II and B-type II amine-functionalized compounds **5** and **6** were reacted with linker **21** in the presence of DIPEA under similar conditions (Scheme 5) to provide the Fmoc-protected adducts. Deprotection with 20% piperidine in DMF afforded compounds **24** and **25** in 72% and 74% yields in two-steps after semi-preparative RP-HPLC purification. Conjugation of compounds **26** and **27** with the NHS-activated PEG **7**, under identical coupling conditions described for conjugate **23**, afforded tetravalent A-type II conjugate **26** (15.7 kDa) and B-type II conjugate **27** (15.5 kDa) in 90% and 94% yields after C-18

purification. Analysis of the ^{1}H NMR spectra and MALDI-TOF mass spectra of **26** and **27** established their tetravalent structure (see Experimental Procedures).

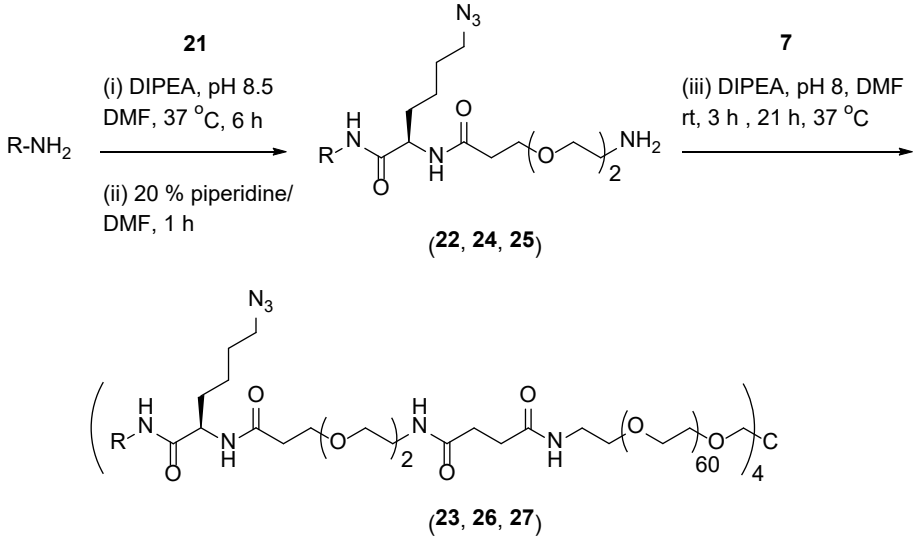

entry	R-NH_2	First amination product	Yield	Second amination product	yield and mol. average weight (kDa)
1	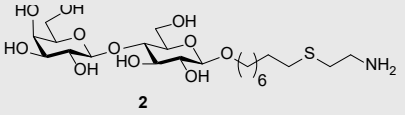	**22**	74%	**23**	(94%, 14.1)
2	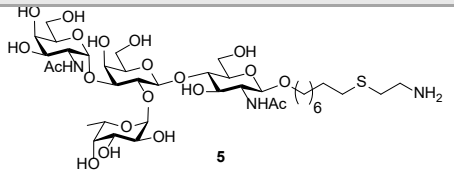	**24**	72%	**26**	(90%, 15.6)
3	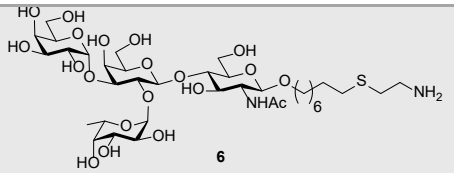	**25**	74%	**27**	(92%, 15.5)

Scheme 5. Synthesis of tetravalent conjugates (**23**, **26**, and **27**) using linker **21**

To conjugate a second glycan, we implemented a CuAAC ligation strategy. This ligation provided octavalent heterobifunctional sialoglycoconjugates (**31**–**39**, 16.7–18.3 kDa), starting from tetravalent platforms **23**, **26**, and **27** (14–15.2 kDa). After several attempts, we

modified the method by Danishefsky and coworkers[98] based on a Cu-powder catalyzed CuAAC reaction in the absence of ligand in PBS buffer (pH 7.4). The tetravalent conjugate **23** was subjected to CuAAC with propargyl sialoglycans including Neu5Ac protected as a C1-methyl ester (**28**), 3'-sialyllactose (3'SL) (**29**) and 6'-sialyllactose (6'SL) (**30**). This coupling generated octavalent sialoglycoconjugates **31**–**39** in good yields and purity (Scheme 6). Monosaccharide **28** was derived in four steps from *N*-acetyl neuraminic acid following a known protocol.[99] The synthesis of propargyl 3'- and 6'-sialeyllactose (**29** and **30**) was achieved in excellent yields using the one-pot chemoenzymatic sialylation protocol (see Experimental Procedures) developed by Chen and coworkers.[100] The CuAAC ligation of conjugate **23** displaying four azide groups to **28** (1.25 equiv per N_3), was carried out in the presence of Cu-powder (10 equiv per N_3) in PBS buffer (pH 7.4) under an inert atmosphere. After C-18 purification, we isolated conjugate **31** (15.5 kDa) in 79% yield. Complete substitution was confirmed from the ^{1}H NMR spectrum. Importantly, the coupling between the carboxylic acid derivative of **28** and **23** was unsuccessful under these conditions. This problem has been reported previously for sialic acids.[45] However, the conjugation between conjugate **23** and propargyl 3'-sialyllactose (**29**) or propargyl 6'-sialyllactose (**30**), both of which possess a free carboxylic acid, proceeded efficiently. Octavalent 3'-sialyllactose conjugate **32** (16.7 kDa) and 3'-sialyllactose conjugate **33** (16.7 kDa) were isolated in 84% and 85% yields using this procedure (Scheme 6). The appearance of triazole peaks at 8.03 ppm (as a broad singlet), NHAc peaks at 1.99 ppm, and analysis of MALDI-TOF mass spectrometry (see Experimental Procedures) established the structure of heterobifunctional glycoconjugates **31–33**.

By employing our CuAAC ligation strategy, conjugate **26** was modified with propargyl sialoglycosides **28**–**30** under CuAAC ligation conditions (Scheme 6). Formation of

the desired A-type II sialoconjugates **34** (17.1 kDa), **35** (18.3 kDa), and **36** (18.1 kDa) was realized in 83%, 85%, and 87% yields, respectively, after C-18 purification. Similar treatment of compound **27** (15.5 kDa) with **28**–**30** afforded the desired B-type II heterofunctional sialoglycoconjugates **37** (16.9 kDa), **38** (18.1 kDa), and **39** (18.1 kDa) in 78–87% yields.

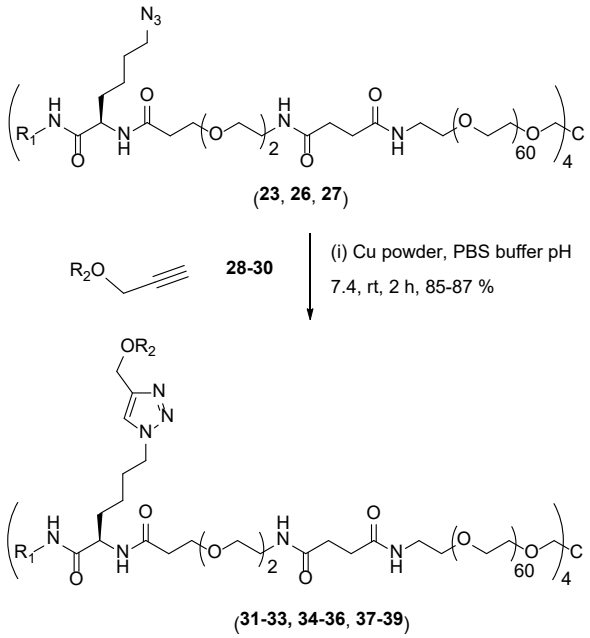

R_2	R_1 = lactose (yield, MW)	R_1 = A-type II (yield, MW)	R_1 = B-type II (yield, MW)
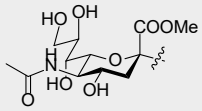	**31** (79%, 15.5)	**34** (79%, 17.0)	**37** (78%, 16.6)
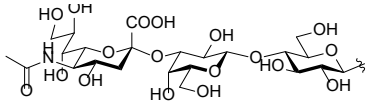	**32** (84%, 16.7)	**35** (86%, 18.3)	**38** (87%, 18.1)
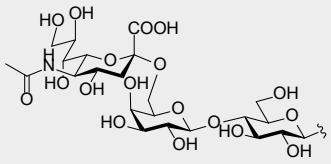	**33** (85%, 16.7)	**36** (84%, 18.3)	**39** (86%, 18.1)

Scheme 6. Conjugation of sialoglycans to tetravalent scaffolds (**23**, **26,** and **27**) using CuAAC ligation

Clustering of BCR and CD22 receptors on B cells. To investigate the ability of conjugates to interact with cell surface receptors, we examined their ability to cluster the targeted receptors *in vitro*. We chose an established cell line (A-BCL) previously used to characterize ABO-antigen coated nanoparticles.[22, 101] A-BCL cells express a BCR complex that binds both A type I and A type II antigens, but not B antigens.[22] We confirmed that these cells expressed both BCR and CD22 receptors, and proceeded to investigate if the conjugates could influence the distribution of these receptors on the cell surface. Using confocal microscopy, we analyzed the distribution of receptors by counting adjacent pixels as a representation of cluster size. These data were compiled and analyzed for changes in distribution of cluster sizes in Table 1 (see Experimental Procedures and Supporting information). As shown in Figure 2, CD22 was generally in isolated microclusters on untreated cells, while the BCR complex was found in larger, but more sparse clusters. Treatment of cells with a control glycoprotein (alpha-1 acid glycoprotein, AGP)[102] caused no detectable changes in CD22 or BCR organization.[103] Treatment with the monofunctional conjugate **9**, containing four copies of the A-type II antigen, generated large clusters of BCRs (sometimes called capping), but had no detectable effect on CD22 distribution. Similar treatment with the conjugate containing four copies of lactose (**33**) caused no detectable changes in the distribution of either receptor. Conjugate **36**, which contained four copies of the A type II antigen and four copies of the 6'-sialyllactose was able to generate a large capping of BCR receptors on the cells. The CD22 receptors on these cells were also found in larger clusters, but fewer receptors were seen at the membrane, which may result from endocytosis upon receptor engagement.[104] We tested other homo- and heterofunctional glycoconjugates to understand the factors influencing clustering of each receptor (see Table 1). A polyacrylic acid polymer bearing sialic acid (PAA) was able to cluster only CD22, but had no effect on BCR

organization. Clustering of the BCR was antigen specific, and in all cases required the presentation of the A-type II antigen (**9**, **34**, **35**, and **36**). The clustering of CD22 required the presentation of a sialoside; however, the nature of its presentation was critical. The 6'-sialyllactose in a tetravalent presentation (**33**) was not sufficient to cluster CD22 without an appropriate BCR ligand (**36**). Furthermore, tetravalent presentation of the sialic acid monosaccharide or 3'-sialyllactoside was unable to cluster CD22 (**34** and **35**). This deficiency could be overcome by a high copy number polymer displaying only sialic acid (PAA, approximately 30 copies based on average molecular weight). We investigated whether the clustering of CD22 and BCR by compound **36** resulted in co-localization of the receptors in a two-color experiment with the same cells (Figure 3). These experiments confirmed distinct co-clustering of BCR and CD22 after treatment of cells with hetero-bifunctional conjugate **36** (see Supporting Information). Superresolution imaging of CD22 and BCR has concluded that CD22 is pre-organized in nanoclusters with high mobility which dynamically associate with BCR,[105] we speculate that the branched scaffolds used in our conjugates may keep the BCR more accessible to these dynamic associations. Together, these results confirmed that the conjugates synthesized in this work can enforce co-clustering of CD22 and BCR on individual cells. Future studies will address the effect of these reagents on the development of antibody response from B cells *in vivo*.

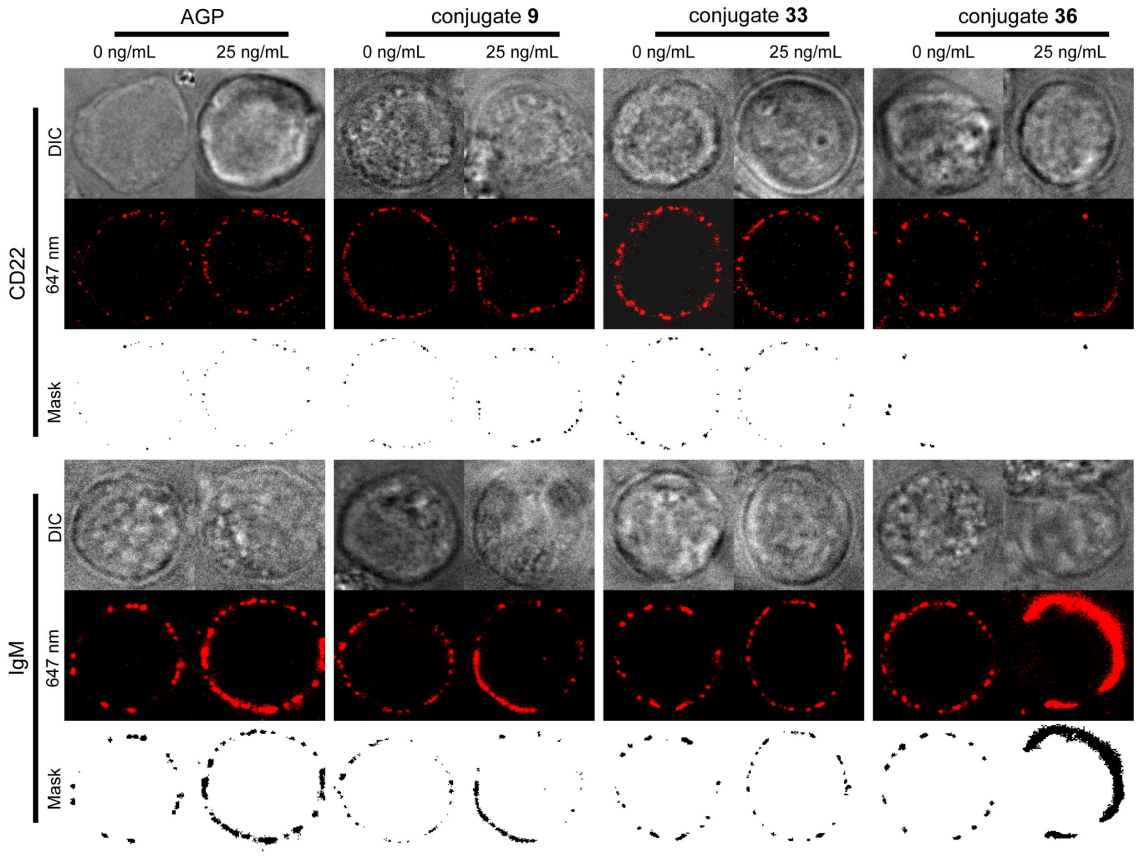

Figure 2: Clustering of BCR and CD22 by heterofunctionalized conjugates. A-BCL cells were treated with the indicated conjugates and observed for changes in the distribution of receptors by confocal microscopy. Each condition is shown with a negative control, or after treatment with the compound indicated. Cells were treated for 30 min at 37 °C, followed by fixing and staining before imaging.

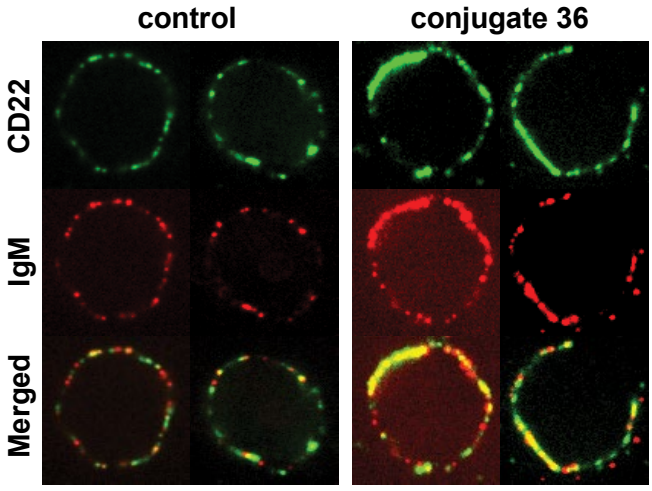

Figure 3: Co-localization of BCR and CD22 by heterofunctionalized conjugates. A-BCL cells were treated with 0 or 25 ng mL^{-1} of conjugate **36**, fixed and stained with anti-IgM (rabbit) and anti-CD22 (mouse) and appropriate secondary antibodies (goat anti-rabbit Alexa Fluor 543; goat anti-mouse Alexa Fluor 647). The samples were imaged by confocal microscopy at 60X magnification. A representative set of cells are show, and co-localization was quantified using multiple fields in two separate experiments (see Supporting information).

Table 1: Clustering of BCR and CD22 receptors by conjugates and proteins

Compound	*Name/Antigen*[a]	*IgM*[b]	*n*	*cluster*[c]	*CD22*[b]	*n*	*cluster*[c]
-	control	0.32 ± 0.04	159	-	0.08 ± 0.004	127	-
-	AGP	0.36 ± 0.03	144	-	0.10 ± 0.01	56	-
-	PAA(SA)	0.29 ± 0.02	155	-	0.21 ± 0.06	84	+
8	4(Lac)	0.28 ± 0.02	143	-	0.11 ± 0.01	119	-
9	4(AII)	1.3 ± 0.2	55	+	0.10 ± 0.02	32	-
10	4(BII)	0.33 ± 0.03	194	-	0.11 ± 0.01	109	-
33	4(Lac)4(6'SL)	0.24 ± 0.02	139	-	0.07 ± 0.01	44	-
34	4(AII)4(SA)	0.93 ± 0.18	80	+	0.12 ± 0.01	161	-
35	4(AII)4(3'SL)	0.83 ± 0.13	98	+	0.13 ± 0.01	159	-
36	4(AII)4(6'SL)	2.2 ± 0.5	57	+	0.6 ± 0.2	45	+

a. Antigens on synthetic conjugates are listed in parenthesis, with the copy number preceding. Abbreviations used are: alpha-1 acid glycoprotein, AGP; sialic acid, SA; lactose, Lac; A-type II, AII; B-type II, BII; 6'-sialyllactose, 6'SL; 3'-sialyllactose, 3'SL.

b. Mean cluster size [μm^2] of the indicated receptor was determined as described in materials and methods.

c. The value of n refers to the number of individual clusters detected in the images from 10 cells for each condition. If the mean cluster size was statistically larger ($p < 0.0001$ by the Student's t-test) for the indicated receptor after treatment with a protein or conjugate, it is indicated with a "+".

CONCLUSIONS

In this work, we report a straightforward and efficient conjugation strategy that can be used with amine coupling alone or in combination with a trifunctional linker strategy for orthogonal CuAAC ligation to generate complex and well-defined multivalent neoglycoconjugates in good yields. The resulting conjugates are of high molecular weight, and provide excellent control of the copy number of antigens per molecule. We first demonstrated that the amine coupling enabled an efficient one-step conjugation of carbohydrate epitopes including lactose, A-type II HBGA, and B-type II HBGA to well-defined PEG scaffolds generating tetravalent homogenous glycoconjugates. We also

developed a route to produce AlexaFluor-labeled glycoconjugates using an iterative amine coupling strategy. Moreover, we developed a heterotrifunctional linker for the efficient conjugation of diverse carbohydrate structures such as lactose, A-type II and B-type II HBGA to be attached along with sialoglycans such as Neu5Ac, 3'-sialyllactose, and 6'-linked sialyllactose to a PEG scaffold via sequential dual amine coupling and orthogonal CuAAC ligation. The conjugation strategy offers a promising route for the synthesis of diverse carbohydrate antigens containing sialoglycoconjugate structures, and can be generalized for conjugation of other biomolecules. Finally, we confirmed that these conjugates altered the distribution of BCR and CD22 receptors on B cells *in vitro*, and were able to enforce co-clustering of these two target receptors on cells. Future work will use these tools in investigation of their effects on HBGA-reactive B cells *in vivo*.

EXPERIMENTAL PROCEDURES

General Methods. Reagents were purchased from commercial sources as noted and used without additional purification. A polyacrylic acid polymer conjugate with Neu5Ac (sialic acid, SA; with a propyl linker) was obtained from GlycoTech; which had a molecular weight of 30 kDa, and carbohydrate content of 20 mol%. NHS-activated PEG scaffolds **7** and **8** were obtained from a commercial source (Laysan Bio Inc, Arab, Alabama). Cysteamine hydrochloride, Fmoc-Lys-OH, Cu-powder (<425 μm) and DIPEA were purchased from Sigma-Aldrich, Canada. Fmoc-9-amino-4,7-dioxanonanoic acid was purchased from ChemPep Inc. HBTU and 2-chlorotrityl chloride resins were purchased from Novabiochem. Chloroform-d_1 and D_2O were purchased from Deutero GmbH. Other solvents (analytical and HPLC grade) and reagents were purchased from Aldrich and were used as received. Reactions were conducted under a stream of argon at ambient temperature, unless otherwise

noted, and reactions were monitored by analytical TLC on silica gel 60-F254 (0.25 nm, Silicycle, QC, Canada). Developed TLC plates were visualized under UV lamp (λ_{max} = 254 nm) and charred by heating plates that were dipped in ninhydrin solution in ethanol, and acidified anisaldehyde solution in ethanol. Reaction products were purified by silica gel column chromatography (230-400 mesh, Silicycle, QC, Canada) or size exclusion chromatography using Bio-Gel P-2 Gel from Bio-Rad Laboratories (Canada) Ltd. Ontario, Canada, or C-18 Sep-pak chromatography using ethyl acetate/hexane, or CH_2Cl_2/MeOH and MeOH/H_2O as the mobile phase, respectively. Purifications were also performed by semi-preparative RP-HPLC with a Waters Delta 600 pump, and a Waters 600 controller with Empower 2 software. Eluted peaks were detected with a Waters 2420 evaporative light scattering (ELS) detector or a Waters 2996 photodiode array (PDA) detector (Waters Ltd., Mississauga, ON, Canada). Purifications were performed using solvent A: 0.01% TFA in water and solvent B: in CH_3CN at flow rate of 8.0 mL min^{-1} using a linear gradient of 2–50% solvent B in 20 min and UV detection at 214 nm. NMR experiments were conducted on a Varian 400, 500, or 600 MHz instruments in the University of Alberta Chemistry NMR Facility. Chemical shifts are reported relative to the deuterated solvent peak or 3-(trimethylsilyl)-propionic-2,2,3,3-d_4 acid sodium salt as an internal standard and are in parts per million (ppm). Coupling constants (*J*) are reported in Hz and apparent multiplicities were described in standard abbreviations as singlet (s), doublet (d), doublet of doublets (dd), triplet (t), broad singlet (bs), or multiplet (m). The ratio of the incorporated carbohydrate onto the PEG scaffold was estimated by integration of the anomeric peaks (5.30–4.40 ppm), PEG-COCH_2CH_2CO- (s, 2.49 or 2.50 ppm, 4H/per site), NH*Ac* moiety of sialic acid (s, 1.98 or 1.99 ppm, 3H) and aromatic peaks of the fluorescent dye protons in ^{1}H NMR spectra. Electrospray mass spectra (ESI-MS) were recorded on Agilent Technologies 6220 TOF.

MALDI-TOF Mass spectrometry analysis. Samples were dissolved in water and an aliquot of 1 μL of sample was spotted onto a Bruker Daltonics MTP ground steel target and air dried. A 1 μL aliquot of matrix solution was spotted on top of the sample spot and air dried. The matrix solution consisted of a saturated solution of CHCA (α-cyano-4-hydroxycinnamic acid) or DHB (dihydroxybenzoic acid) in 50% water acetonitrile with 0.1% TFA. Mass spectra were obtained in the positive or negative linear mode of ionization using a Bruker Daltonics (Bremen, Germany) ultrafleXtreme MALDI TOF/TOF mass spectrometer. Data Analysis software packages provided by the manufacturer was used for analysis.

General procedure for fluorescent conjugates. A mixture of AlexaFluor 488 dye (0.5–1.0 equiv) and NHS-activated PEG scaffold (**7**, 10 mg, 1 equiv) were dissolved in anhydrous DMF (~100 μL) with DIPEA and placed in a 0.5 mL centrifuge tube at room temperature. Consumption of the AlexaFluor 488 and progress of the conjugation was monitored by TLC. After ~3 h, the carbohydrate amine (3.0-3.5 equiv) was added, and the reaction was again purged with argon, and kept at room temperature for an additional ~21 h. The solvent was removed and the crude product was purified by C_{18} Sep-pak chromatography using gradient elution of H_2O to MeOH/H_2O (3:2, v/v) to afford florescent-labeled conjugate as a redish colored powder after lyophilization.

General procedure for CuAAC ligation. A solution of azide terminated PEG-conjugate (1 equiv) and propargyl glycoside (1.25 equiv per N_3) in PBS buffer (5 mM, pH 7.4) was degassed at room temperature under an argon atmosphere for ~20 min. Cu-power (10 equiv per N_3) was added to the reaction mixture under an argon atmosphere and the reaction mixture was vigorously stirred for another ~2 h at room temperature. The progress of the coupling was monitored by TLC for disappearance of the propargyl compounds. The solution

was filtered through a two-micron filter and the crude product was purified by C_{18} Sep-pak chromatography using H_2O to MeOH/H_2O eluent to afford the conjugate as a colorless powder after lyophilization.

8-[(2-Aminoethyl)thiol)]-1-octyl-β-D-galactopyranosyl-(1→4)-β-D-glucopyranoside (2). Compound **1** (10 mg, 0.24 mmol) and cysteamine hydrochloride salt (27.2 mg, 0.024 mmol) were dissolved in anhydrous MeOH (0.5 mL) in a quartz tube. The solution was degassed and the tube was filled with argon. The reaction mixture was irradiated under UV light for 45 min, the solution was concentrated and the crude mixture was purified by C_{18} Sep-pak chromatography using gradient elution (0.5% aq AcOH to 1:8 v/v MeOH/0.5% aq AcOH) followed by treatment with Dowex resin (HO^-) afforded the amine **2** (10.4 mg, 89 %). ^{1}H NMR (600 MHz, D_2O): δ 4.43 (d, *J* = 7.8, 1H, H-1'), 4.40 (d, *J* = 7.8, 1H, H-1), 3.93 (dd, *J* = 10.8, 1.2 Hz, 1H), 3.88-3.85 (m, 2H), 3.75 (dd, *J* = 10.8, 4,2 Hz, 1H), 3.72 (dd, *J* = 10.8, 4.2 Hz, 1H), 3.69-3.67 (m, 2H), 3.66-3.59 (m, 4H), 3.55-3.54 (m, 1H, C*H*$_2$), 3.50 (dd, *J* = 9.6, 7.8 Hz, 1H,), 3.26 (t, *J* = 8.4 Hz, 1H, C*H*$_2$), 3.09 (t, *J* = 6.6 Hz, 2H, C*H*$_2$), 2.76 (t, *J* = 6.6 Hz, 2H, C*H*$_2$), 2.55 (t, *J* = 7.2 Hz, 2H, C*H*$_2$), 1.59-1.53 (m, 4H, C*H*$_2$), 1.35-1.28 (m, 8H, C*H*$_2$); ^{13}C NMR (126 MHz, D_2O): δ 103.91, 102.99, 79.44, 76.35, 75.74, 75.46, 73.84, 73.53, 71.95, 71.70, 62.01, 61.11, 39.37, 31.71, 29.66, 29.52, 29.25, 29.10, 28.80, 28.75, 25.92, 24.03. HRMS (ESI): m/z $[M+H]^+$ calcd for $C_{22}H_{43}NO_{11}S$: 530.2630, found: 530.2629.

8-[(2-Aminoethyl)thiol)]-1-octyl-2-acetamido-2-deoxy-4-*O*-(2-O-(α-L-fucopyranosyl)-3-*O*-(2-acetamido-2-deoxy-α-D-galactopyranosyl)-β-D-galactopyranosyl)-2-deoxy-β-D-glucopyranoside (5). Compound **5** was obtained through irradiation of compound **3** (10 mg, 0.01 mmol) and cysteamine hydrochloride (13.4 mg, 0.11 mmol) in dry MeOH (1 mL) under UV light by following the procedure for compound **2**. The crude mixture was purified by C_{18}

Sep-pak chromatography using gradient elution (0.5% aq. AcOH to 2:8 v/v MeOH/0.5% aq AcOH), followed by treatment with HO^- resin afforded the amine **5** (9.5 mg, 87 %). ^{1}H NMR (600 MHz, D_2O): δ 5.30 (d, *J* = 3.6 Hz, H-1", 1H), 5.13 (d, *J* = 3.6 Hz, H-1"', 1H), 4.55 (d, *J* = 7.8 Hz, H-1', 1H), 4.44 (d, *J* = 8.4 Hz, H-1, 1H), 4.27 (q, *J* = 6.6 Hz, 1H), 4.20-4.15 (m, 3H), 3.95-3,92 (m, 3H), 3.85-3.83 (m, 3H), 3.79-3.71 (m, 11H), 3.66-3.60 (m, 1H), 3.59-3.55 (m, 1H, C*H*$_2$-), 3.41-3.28 (m, 1H, C*H*$_2$-), 3.16 (t, *J* = 6.6 Hz, 2H, C*H*$_2$-), 2.79 (t, *J* = 6.6 Hz, 2H, C*H*$_2$-), 2.55 (t, *J* = 7.2 Hz, 2H, C*H*$_2$-), 1.99 (s, 6H), 1.55-1.53 (m, C*H*$_2$-, 2H), 1.49 (t, *J* = 6.6 Hz, C*H*$_2$-, 2H), 1.33 (t, *J* = 6.6 Hz, C*H*$_2$-, 2H), 1.26 (bs, C*H*$_2$-, 6H), 1.18 (d, *J* = 6.6 Hz, 3H); ^{13}C NMR (126 MHz, D_2O): δ 175.78, 175.34, 102.11, 101.05, 99.62, 92.31, 77.24, 76.66, 76.33, 76.15, 73.42, 73.41, 72.70, 72.07, 71.65, 70.95, 69.48, 68.78, 68.66, 67.83, 64.02, 62.30, 62.17, 61.20, 56.40, 39.40, 31.71, 29.55, 29.52, 29.25, 29.24, 29.21, 28.80, 26.02, 23.25, 22.93, 16.15, 16,14; HRMS (ESI): m/z $[M+H]^+$ calcd for $C_{38}H_{70}N_3O_{20}S$: 920.4268, found: 920.4270.

8-[(2-Aminoethyl)thiol)]-1-octyl-2-acetamido-2-deoxy-4-*O*-(2-O-(α-L-fucopyranosyl)-3-*O*-(α-D-galactopyranosyl)-β-D-galactopyranosyl)-2-deoxy-β-D-glucopyranoside (6). Compound **6** was obtained through irradiation of compound **4** (10 mg, 0.01 mmol) and cysteamine hydrochloride (14.2 mg, 0.12 mmol) in anhydrous MeOH (1 mL) under UV light by following the procedure for compound **2**. The crude mixture was purified by C_{18} Sep-pak chromatography using gradient elution (0.5% aq AcOH to 2:8 v/v MeOH/0.5% aq AcOH), followed by treatment with HO^- resin afforded the amine **6** (9.7 mg, 88 %). ^{1}H NMR (600 MHz, D_2O): δ 5.28 (d, *J* = 4.2 Hz, H-1", 1H), 5.19 (d, *J* = 3.6 Hz, H-1"', 1H), 4.57 (d, *J* = 7.8 Hz, H-1', 1H), 4.44 (d, *J* = 8.4 Hz, H-1, 1H), 4.27-4.23 (m, 2H), 4.15 (t, *J* = 6.0 Hz, 1H), 3.95-3.93 (m, 3H), 3.89-3.84 (m, 3H), 3.79-3.65 (m, 12H), 3.62-3.61 (m, 1H), 3.60-3.50 (m,

CH_2-, 1H), 3.41-3.38 (m, CH_2-, 1H), 3.10 (t, J = 6.6 Hz, CH_2-, 2H), 2.77 (t, J = 6.6 Hz, CH_2-, 2H), 2.55 (t, J = 7.2 Hz, CH_2-, 2H), 1.99 (s, 3H), 1.57-1.54 (m, CH_2-, 2H), 1.49 (t, J = 6.6 Hz, CH_2-, 2H), 1.34 (t, J = 6.6 Hz, CH_2-, 2H), 1.26 (bs, CH_2-, 6H), 1.18 (d, J = 6.6 Hz, 3H); ^{13}C NMR (126 MHz, D_2O): δ 175.34, 102.13, 101.10, 99.75, 94.03, 77.21, 77.19, 76.31, 75.92, 73.53, 73.42, 72.69, 72.13, 71.64, 71.0, 70.49, 70.26, 69.04, 68.68, 67.76, 64.49, 62.26, 62.13, 61.20, 56.35, 39.58, 31.73, 29.98, 29.58, 29.51, 29.25, 29.20, 28.80, 26.01, 23.25, 16.14. HRMS (ESI): m/z $[M+H]^+$ calcd for $C_{36}H_{67}N_2O_{20}S$: 879.4002, found: 879.3998.

Synthesis of conjugate 8. Conjugate **8** was obtained by conjugation of compound **2** (2.26 mg, 4.28 μmol) to NHS-activated PEG **7** (8 mg, 0.71 μmol) in anhydrous DMF (150 μL) at room temperature under anhydrous conditions. DIPEA (2 equiv.) was added to the solution to adjust pH ~8.0 and the reaction mixture was incubated at room temperature for 2 h and then incubated at 37 ^{o}C. After ~24 h, the solvent was removed, and the resulting crude reaction mixture was purified by C_{18} Sep-pak chromatography using gradient elution 0.1 % aq. AcOH to 7:3 MeOH/H_2O to afford conjugate **8** (8.5 mg, 92 %) as a colorless power after lyophilization. Substitution of the PEG scaffold was determined by ^{1}H NMR integration of the underlined peaks to be lactose:PEG = 4:1. ^{1}H NMR (600 MHz, D_2O): δ <u>4.43</u> (d, J = 7.8 Hz, 1H), <u>4.40</u> (d, J = 7.8 Hz, 1H), 3.93 (dd, J = 12.6, 1.8 Hz, 1H), 3.88-3.85 (m, 2H), 3.78-3.76 (m, 2H), 3.75-3.69 (m, 2H), 3.66 (band, PEG CH_2-, 237H), 3.63-3.57 (m, 20H), 3.54-3.53 (m, 2H), 3.50 (dd, J = 7.8, 10.2 Hz, 1H), 3.46 (bs, 2H), 3.34 (t, J = 6.0 Hz, 4H), 3.30-3.24 (m, 1H), 2.64 (t, J = 6.6 Hz, 2H), 2.54 (t, J = 7.2 Hz, 2H), <u>2.49</u> (bs, PEG-COCH_2CH_2CO- , 4H), 1.59-1.53 (m, 4H), 1.35-1.28 (m, 8H);; ^{13}C NMR (126 MHz, D_2O): δ 175.65, 175.59, 103.92, 103.03, 79.43, 76.34, 75.74, 75.47, 73.84, 73.53, 71.95, 71.68, 71.57, 70.58 (PEG C), 70.41, 69.83, 69.54, 62.0, 61.12, 46.05, 39.97, 39.72, 32.22, 32.20, 32.06, 31.36, 29.72, 29.33, 29.16, 28.85, 25.98; The MALDI-TOF spectrum showed the average

mass ion centered at 12.8 kDa with clearly visible PEG repeating unit (44 Da) over the peak and expected average mass was12.8 kDa.

Synthesis of conjugate 9. Conjugate **9** was obtained from compound **5** (3.94 mg, 4.28 μmol) and NHS-activated PEG **7** (8 mg, 0.71 μmol) in dry DMF (150 μL) following the procedure described for conjugate **8**. Yield: (9.55 mg, 92%); Substitution of the PEG scaffold was determined by ^{1}H NMR integration of the underlined peaks to be A-type II:PEG= 4:1. ^{1}H NMR (600 MHz, D_2O): δ 5.30 (d, *J* = 4.2 Hz, 1H), 5.13 (d, *J* = 4.2 Hz, 1H), 4.55 (d, *J* = 7.8 Hz, 1H), 4.45 (d, *J* = 8.4 Hz, 1H), 4.27(dd, *J* = 13.2, 6.6 Hz, 1H), 4.19 (dd, *J* = 11.4, 1.8 Hz, 1H), 4.18-4.16 (m, 2H), 3.95-3.92 (m, 3H), 3.87-3.83 (m, 3H), 3.79-3.77 (m, 4H), 3.75-3.71 (m, 6H), 3.66 (band, PEG C*H*$_2$-, 252H), 3.57 (t, *J* = 6.0, 2H), 3.54-3.51 (m, 2H), 3.46 (bs, 2H), 3.40-3.37 (m, 1H), 3.34 (t, *J* = 6.0 Hz, 4H), 2.64 (t, *J* = 6.6 Hz, 2H), 2.54 (t, *J* = 7.2 Hz, 2H), 2.49 (bs, PEG-COC*H*$_2$C*H*$_2$CO-, 4H), 1.99 (s, 6H), 1.55-1.50 (m, 4H), 1.35-1.31 (m, 2H), 1.26(bs, 7H), 1.20 (d, *J* = 6.6 Hz, 3H); ^{13}C NMR (126 MHz, D_2O): δ 175.78, 175.66, 175.60, 175.27, 102.09, 101.05, 99.62, 92.31, 77.26, 76.66, 76.15, 73.40, 72.69, 72.07, 71.57, 70.94, 70.58 (PEG C*H*$_2$-), 69.83, 70.41, 69.83, 68.48, 68.78, 68.66, 67.83, 64.02, 62.29, 62.16, 61.21, 56.42, 50.50, 46.05, 39.97, 39.71, 32.20, 32.19. 32.05, 31.30, 29.72, 29.54, 29.30, 29.25, 28.88, 26.04, 23.27, 22.94, 16.16; The MALDI-TOF spectrum showed the average mass centered at 14.4 kDa with clearly visible PEG repeating unit (44 Da) over the peak and expected average mass was 14.4 kDa.

Synthesis of conjugate 10. Compound **6** (4.23 mg, 4.82 μmol) and NHS-activated PEG **7** (9 mg, 0.89 μmol) were dissolved in anhydrous DMF (160 μL) at room temperature followed by the procedure for conjugate **8** afforded conjugate **10** (10.7 mg, 94 %) as white amorphous power after C_{18} Sep-pak chromatographic purification using solvent gradient elution 1-80% MeOH/H_2O and lyophilization. Substitution of the PEG scaffold was determined by ^{1}H NMR

integration of the underlined peaks to be B-type II:PEG = 4:1. ^{1}H NMR (600 MHz, D_2O): δ 5.28 (d, *J* = 3.6 Hz, 1H), 5.19 (d, *J* = 1.8 Hz, 1H), 4.57 (d, *J* = 7.8 Hz, 1H), 4.44 (d, *J* = 8.4 Hz, 1H), 4.27-4.26 (m, 1H), 4.23 (d, *J* = 1.8 Hz, 1H), 4.15 (t, *J* = 6.0 Hz, 1H), 3.96-3.92 (m, 3H), 3.89-3.84 (m, 4H), 3.77-3.73 (m, 4H), 3.66 (band, PEG C*H*$_2$-, 254H), 3.62-3.61 (m, 4H), 3.57 (t, *J* = 5.4 Hz, 2H), 3.54-3.52 (m, 2H), 3.45 (bs, 2H), 3.41-3.64 (m, 1H), 3.34 (t, *J* = 6.0 Hz, 4H), 2.64 (t, *J* = 6.0 Hz, 2H), 2.54 (t, *J* = 7.8 Hz, 2H), 2.49 (bs, PEG-COC*H*$_2$C*H*$_2$CO-, 4H), 1.99 (s, 3H), 1.55-1.49 (m, 4H), 1.35-1.29 (m, 2H), 1.26 (bs, 7H), 1.19 (d, *J* = 6.6 Hz, 3H); ^{13}C NMR (126 MHz, D_2O): 175.66, 175.60, 175.26, 102.12, 101.10, 99.76, 94.03, 77.24, 77.20, 76.32, 75.92, 73.52, 73.40, 72.69, 72.13, 71.57, 71.56, 70.99, 70.58 (PEG C*H*$_2$-), 70.41, 70.26, 69.83, 69.04, 68.68, 67.77, 64.49, 62.25, 62.12, 61.21, 56.37, 39.97, 39.72, 32.21, 32.19, 32.05, 31.36, 29.72, 29.54, 29.31, 29.26, 29.26, 28.88, 26.04, 23.27, 16.16; The MALDI-TOF spectrum showed the average mass centered at 14.2 kDa with clearly visible PEG repeating unit (44 Da) over the peak and expected average mass was 14.2 kDa

Synthesis of conjugate 12. Compound **2** (2.26 mg, 4.28 μmol) and NHS-activated PEG **11** (8 mg, 0.71 μmol) were dissolved in anhydrous DMF (150 μL) at room temperature under an argon atmosphere followed by the procedure for conjugate **8**. After ~24 h, the solvent was removed, and the resulting crude reaction mixture was purified by C_{18} Sep-pak chromatography using gradient elution 0.1 % aq. AcOH to 7:3 MeOH/H_2O to afford conjugate **12** (8.5 mg, 92 %) as white power after lyophilization. Substitution of the PEG scaffold was determined by ^{1}H NMR integration of the underlined peaks to be lactose:PEG = 4:1. ^{1}H NMR (600 MHz, D_2O): δ 4.43 (d, *J* = 7.8 Hz, 1H), 4.40 (d, *J* = 7.8 Hz, 1H), 3.93 (dd, *J* = 12.6, 2.4 Hz, 1H), 3.88-3.85 (m, 2H), 3.78-3.76 (m, 2H), 3.75-3.71 (m, 2H), 3.66 (band, PEG C*H*$_2$-, 250H), 3.63-3.61 (m, 3H), 3.60-3.53 (m, 4H), 3.56-3.51 (m, 2H), 3.50 (dd, *J* = 7.8, 9.6 Hz, 1H), 3.46 (bs, 2H), 3.34 (t, *J* = 6.0 Hz, 4H), 3.27-3.24 (m, 1H), 2.64 (t, *J* = 6.6

Hz, 2H), 2.54 (t, *J* = 7.2 Hz, 2H), 2.49 (bs, PEG-COC*H*$_2$C*H*$_2$CO-, 4H), 1.60-1.52 (m, 4H), 1.33-1.28 (m, 8H); ^{13}C NMR (126 MHz, D_2O): δ 175.65, 175.59, 103.92, 103.03, 79.43, 76.34, 75.75, 75.47, 73.84, 73.53, 71.95, 71.68, 71.57, 70.58 (PEG *C*), 70.41, 69.83, 69.54, 62.0, 61.12, 39.97, 39.72, 32.22, 32.20, 32.06, 31.36, 29.72 (2Cs), 29.33, 29.16, 28.85, 25.98; MALDI-TOF spectrum showed the average mass centered at 12.8 kDa with clearly visible PEG repeating unit (44 Da) over the peak and expected average mass was 12.8 kDa.

Synthesis of conjugate 13. Conjugate **13** was obtained from compound **5** (3.94 mg, 4.28 μmol) and NHS-activated PEG **11** (8 mg, 0.71 μmol) in anhydrous DMF (160 μL) following the procedure described for conjugate **8**. Yield: (9.61 mg, 93%); Substitution of the PEG scaffold was determined by ^{1}H NMR integration of the underlined peaks to be A-type II:PEG = 4:1. ^{1}H NMR (600 MHz, D_2O): δ 5.30 (d, *J* = 4.2 Hz, 1H), 5.13 (d, *J* = 3.6 Hz, 1H), 4.55 (d, *J* = 7.8 Hz, 1H), 4.45 (d, *J* = 8.4 Hz, 1H), 4.29-4.26 (m, 1H), 4.19 (dd, *J* = 10.8, 1.8 Hz, 1H), 4.18-4.16 (m, 2H), 3.95-3.92 (m, 3H), 3.87-3.83 (m, 3H), 3.79-3.73 (m, 7H), 3.71-3.69 (m, 2H), 3.68-3.63 (band, PEG C*H*$_2$-, 249H), 3.63-3.61 (m, 4H), 3.57 (t, *J* = 5.4 Hz, 2H), 3.54-3.51 (m, 2H), 3.45 (bs, 2H), 3.40-3.37 (m, 1H), 3.34 (t, *J* = 6.0 Hz, 4H), 2.64 (t, *J* = 6.6 Hz, 2H), 2.54 (t, *J* = 7.2 Hz, 2H), 2.49 (bs, PEG-COC*H*$_2$C*H*$_2$CO-, 4H), 1.99 (s, 6H), 1.56-1.49 (m, 4H), 1.34-1.32 (m, 2H), 1.26 (bs, 7H), 1.20 (d, *J* = 6.6 Hz, 3H); ^{13}C NMR (126 MHz, D_2O): δ 175.78, 175.65, 175.60, 175.27, 102.09, 101.05, 99.62, 94.31, 77.26, 76.67, 76.35, 76.15, 73.40, 72.70, 72.07, 71.57, 70.94, 70.58 (PEG C*H*$_2$-), 69.83, 69.49, 68.79, 68.67, 67.83, 64.03, 62.30, 62.17, 61.21, 50.50, 49.60, 46.05, 39.97, 39.72, 32.21. 32.20, 32.05, 31.36, 29.72, 29.54, 29.30, 29.26, 28.88, 26.04, 23.28, 22.94, 16.16; The MALDI-TOF spectrum showed the average mass centered at 14.4 kDa with clearly visible PEG repeating unit (44 Da) over the peak and expected average mass was 14.4 kDa.

Synthesis of conjugate 14. Conjugate **14** was obtained on conjugation of compound **6** (3.76 mg, 4.28 μmol) to NHS-activated PEG **11** (8 mg, 0.71 μmol) in anhydrous DMF (150 μL) at room temperature followed by the procedure for conjugate **8**. Yield: (9.5 mg, 93 %) as white amorphous power after lyophilization. Substitution of the PEG scaffold was determined by ^{1}H NMR integration of the underlined peaks to be B-type II:PEG = 4:1. ^{1}H NMR (600 MHz, D_2O): δ 5.28 (d, *J* = 4.2 Hz, 1H), 5.19 (d, *J* = 2.4 Hz, 1H), 4.57 (d, *J* = 7.2 Hz, 1H), 4.47 (d, *J* = 8.4 Hz, 1H), 4.26 (dd, *J* = 13.2, 6.6 Hz, 1H), 4.23 (d, *J* = 3.2 Hz, 1H), 4.15 (t, *J* = 6.0 Hz, 1H), 3.95-3.92 (m, 3H), 3.89-3.83 (m, 4H), 3.78-3.73 (m, 4H), 3.71-3.69 (m, 4H), 3.66 (band, PEG-C*H*$_2$-, 254H), 3.57 (t, *J* = 5.4 Hz, 2H), 3.54-3.51 (m, 2H), 3.45 (bs, 2H), 3.41-3.64 (m, 1H), 3.34 (t, *J* = 6.0 Hz, 4H), 2.64 (t, *J* = 6.0 Hz, 2H), 2.54 (t, *J* = 7.8 Hz, 2H), 2.49 (bs, PEG-COC*H*$_2$C*H*$_2$CO-, 4H), 1.99 (s, 3H), 1.55-1.49 (m, 4H), 1.35-1.30 (m, 2H), 1.29-1.26(m, 7H), 1.19 (d, *J* = 6.6 Hz, 3H); ^{13}C NMR (126 MHz, D_2O): δ 175.66, 175.60, 175.26, 102.12, 101.11, 99.76, 94.03, 77.24, 77.20, 76.32, 75.93, 73.52, 73.41, 72.70, 72.13, 71.58, 71.57, 71.0, 70.58, 70.41 (PEG C*H*$_2$-), 70.26, 69.83, 69.05, 68.69, 67.78, 67.77, 64.50, 62.26, 62.12, 61.21, 56.38, 46.05, 39.98, 39.72, 32.23, 32.22, 32.20, 32.05, 31.36, 29.73, 29.55, 29.31, 29.27, 29.26, 28.88, 26.04, 23.28, 16.16; The MALDI-TOF spectrum showed the average mass centered at 14.2 kDa with clearly visible PEG repeating unit (44 Da) over the peak and expected average mass was 14.2 kDa.

Synthesis of conjugate 16. Conjugate **16** was obtained on treatment of Alexa Fluor 488 cadaverine **15** (0.37 mg, 0.58 μmol, 0.65 equiv) and compound **2** (1.65 mg, 3.12 μmol, 3.5 equiv) with NHS-activated PEG **7** (10 mg, 0.89 μmol, 1 equiv) following the general procedure for fluorescent labeling. Yield: (10.41 mg, 90 %); Substitution of the PEG scaffold was determined by ^{1}H NMR integration of the underlined peaks to be AlexaFlour:lactose:PEG = 1.3:2.7:1. ^{1}H NMR (600 MHz, D_2O): δ 8.26 (s, 0.3H), 8.00 (s,

0.3H), 7.96 (d, *J* = 7.2 Hz, 0.15H), 7. 96 (d, *J* = 7.2 Hz, 0.15H), 7.61 (s, 0.3H), 7.39 (d, *J* = 7.2 Hz, 0.15H), 7.18 (d, *J* = 9.6 Hz, 0.6H), 6.92 (d, *J* = 9.0 Hz, 0.6H), 4.43 (d, *J* = 8.4 Hz, 1H), 4.40 (d, *J* = 7.8 Hz, 1H), 3.93 (dd, *J* = 1.8, 12.0 Hz, 1H), 3.88-3.81 (m, 2H), 3.77-3.57 (bs, 261H), 3.54 (s, 3H), 3.51-3.48 (m, 2H), 3.46 (s, 2H), 3.34 (t, *J* = 6.0 Hz, 3H), 3.27-3.24 (m, 1.3H), 3.16 (t, *J* = 6.6 Hz, 0.9H), 3.11 (t, *J* = 6.6 Hz, 0.3H), 2.95 (t, *J* = 6.0 Hz, 0.3H), 2.80 (t, *J* = 6.6 Hz, 0.6H), 2.64 (t, *J* = 6.6 Hz, 2H), 2.55-2.63 (m, 2H), 2.49 (bs, PEG-COC*H*$_2$C*H*$_2$CO-, 4H), 2.46 (t, *J* = 6.0 Hz, 0.3H), 2.43-2.38 (m, 0.6 H), 1.66-1.64 (m, 0.3H), 1.58-1.53 (m, 4.6H), 1.48-1.46 (m, 0.6H), 1.40-1.39 (m, 0.6H), 1.32-1.28 (m, 8.6H); ^{13}C NMR (126 MHz, D_2O): δ 175.63, 175.57, 156.87, 156.56, 132.98, 120.57, 114.70, 114.52, 103.91, 103.01, 79.42, 76.33, 75.73, 75.45, 73.83, 73.51, 71.93, 71.66, 71.55, 70.56 (PEG C*H*$_2$-), 69.81, 69.52, 61.99, 61.10, 46.04, 39.96, 39.70, 39.34, 32.35, 32.19, 32.04, 31.70, 31.35, 29.70, 29.51, 29.32, 29.25, 29.15, 29.10, 28.84, 28.75, 25.96; The MALDI-TOF spectrum showed the average mass centered at 12.9 kDa and expected average mass was 12.9 kDa

Synthesis of conjugate 17. Conjugate **17** was obtained on treatment of Alexa Fluor 488 cadaverine **15** (0.77 mg, 1.20 μmol, 1.35 equiv) and compound **5** (2.17 mg, 2.36 μmol, 2.7 equiv) with NHS-activated PEG **7** (10 mg, 0.89 μmol, 1 equiv) following the general procedure for fluorescent labeling. Yield: (10.41 mg, 90 %); Substitution of the PEG scaffold was determined by ^{1}H NMR integration of the underlined peaks to be AlexaFlour:A-type II:PEG = 0.6:3.4:1. ^{1}H NMR (600 MHz, D_2O): δ 8.26 (s, 0.1H), 8.00 (s, 0.23H), 7.96 (d, *J* = 7.2 Hz, 0.13H), 7.96 (d, *J* = 7.2 Hz, 0.15H), 7.61 (s, 0.15H), 7.39 (d, *J* = 7.2 Hz, 0.13H), 7.18 (d, *J* = 9.6 Hz, 0.48H), 6.92 (d, *J* = 9.0 Hz, 0.48H), 5.30 (d, *J* = 3.6 Hz, 1H), 5.13 (d, *J* = 3.6 Hz, 1H), 4.55 (d, *J* = 7.8 Hz, 1H), 4.45 (d, *J* = 8.4 Hz, 1H), 4.28 (dd, *J* = 6.0, 13.2 Hz, 1H), 4.20-4.16 (m, 3H), 3.95-3.93 (m, 3H), 3.87-3.83 (m, 3H), 3.78-3.76 (m, 4H), 3.74-3.57 (band,

PEG CH_2-, 278H), 3.54-3.49 (m, 4H), 3.46 (bs, 2H), 3.40-3.37 (m, 1H), 3.34 (t, *J* = 5.4 Hz, 4H), 3.26 (t, *J* = 5.4 Hz, 1.3H), 3.16-3.11 (m, 1.3H), 2.95 (t, *J* = 6.0 Hz, 1.3H), 2.82-2.79 (m, 1.3H), 2.64 (t, *J* = 6.6 Hz, 2H), 2.64 (t, *J* = 7.2 Hz, 2H), 2.49 (bs, PEG-COCH_2CH_2CO-, 4H), 2.42-2.38 (m, 1.3H), 1.99 (s, 6H), 1.67-1.64 (m, 1.3H), 1.55-1.50 (m, 5.3H), 1.40-1.38 (m, 1.3H), 1.35-1.31 (m, 2H), 1.26 (bs, 8.3H), 1.20 (d, *J* = 6.6 Hz, 4.3H); AlexaFlour:A-type II:PEG = 1.3:2.7:1; ^{13}C NMR (126 MHz, D_2O): δ 175.76, 175.63, 175.57, 175.45, 175.24, 156.91, 156.87, 156.58, 156.54, 133.00, 120.58, 114.70, 114.51, 112.47, 102.08, 101.04, 99.61, 92.30, 77.24, 76.65, 76.33, 76.14, 73.38 (2C), 73.03, 72.68, 72.05, 71.55(2C), 70.92, 70.65, 70.57 (PEG CH_2-), 70.40, 69.82, 69.47, 68.76, 68.65, 67.82, 64.01, 63.46, 62.28, 62.18, 61.34, 61.19, 59.84, 56.41, 52.77, 51.99, 50.48, 46.04, 40.89, 40.15, 40.08 (2C), 39.96, 39.70, 32.35, 32.20, 32.18, 32.04, 31.35, 29.72, 29.54, 29.30, 29.25, 29.02, 28.87, 26.03, 24.42, 23.26, 22.93, 16.16; The MALDI-TOF spectrum showed the average mass centered at 14.0 kDa and expected average mass was 14.0 kDa.

Solid-phase synthesis of linker 20. Synthesis of linear dipeptide was accomplished by employing solid phase peptide synthetic protocol starting from Fmoc-Lys(N_3)-OH (**18**) and 2-chlorotrityl chloride resin and using the Fmoc strategy. Coupling reactions were performed using 2-chlorotrityl chloride resin (500 mg, 0.65 mmol) and Fmoc-amino acids **19** (3 equiv) in the presence of HBTU (2 equiv) and DIPEA (3 equiv) in CH_2Cl_2 and DMF (10 mL g^{-1} resin), respectively, for 45 min. After each reaction the resin beads were repeatedly washed with DMF (10 mL, 4 times) to remove excess amino acids and coupling reagent. Progress of the coupling reaction was monitored by the TNBS test using a solution of trinitrobenzenesulfonic acid in DMF (1%). The *N*-Fmoc protecting group was removed by treatment with 20 % piperidine-DMF (10 mL 1:4, v/v, g^{-1} resin) for 15 min. The linear peptides were cleaved from resins treated with cleavage cocktail TFA: H_2O: TIPS (4X2 mL,

9:0.5:0.5) for 2 h. The combined cleavage solutions were concentrated under vacuum and the crude product was purified by silica gel chromatography using ethyl acetate as eluent to afford peptide **20** (400 mg, 79%) as colorless oil. R_f = 0.41 (EtOAc/MeOH = 9.5:0.5); ^{1}H NMR (600 MHz, $CDCl_3$): δ 7.77 (d, *J* = 7.2 Hz, aromatic H, 2H), 7.61 (d, *J* = 7.2 Hz, aromatic H, 1H), 7.57 (d, *J* = 7.2 Hz, aromatic H, 1H), 7.40 (d, *J* = 7.2 Hz, aromatic H, 2H), 7.31 (d, *J* = 7.2 Hz, aromatic H, 2H), 7.13 (bs, N*H*-, 1H), 5.61 (s, 1H), 4.58 (bs, 1H), 4.43 (q, *J* = 6.0 Hz, 2H), 4.25-4.22 (m, 1H), 3.72-3.73 (m, 2H), 3,61 (bs, 2H), 3.55 (bs, 2H), 3.52-3.48 (m, 2H), 3.38-3.32 (m, 2H), 3.25-3.23 (m, 2H), 2.56-2.52 (m, 2H), 1.90 (bs, 1H), 1.72 (bs, 1H), 1.59-1.57 (m, 2H), 1.43-1.42 (m, 2H); ^{13}C NMR (126 MHz, $CDCl_3$): δ 171.91, 171.85, 162.66, 156.70, 143.84, 141.26, 127.65, 127.01, 124.88, 119.97, 70.34, 70.00, 66.93, 66.72, 51.10, 51.05, 47.17, 40.78, 36.70, 36.50, 31.53, 28.36, 22.36; HRMS (ESI): m/z $[M+Na]^+$ calcd for $C_{28}H_{34}N_5O_7$-H: 552.2464, found: 552.2464.

Synthesis of heterobifunctional linker 21. *N*-Hydroxysuccinimide (91.5 mg, 0.79 mmol) was added to a solution of linker **20** (400 mg, 0.72 mmol) and *N,N*-dicyclohexylcarbodiimide (164 mg, 0.79 mmol) in CH_2Cl_2 (10 mL) under an argon atmosphere at room temperature. The solution was filtered through celite pad, washed with aq. HCl (2N) solution, dried over sodium sulfate and concentrated under vaccum. The crude product was purified by silica gel chromatography using ethyl acetate-hexane system (2:3) to provide linker **21** (405 mg, 86 %) as colorless oil. R_f = 0.31 (cyclohexane/EtOAc = 3:2); ^{1}H NMR (600 MHz, $CDCl_3$): δ 7.77 (d, *J* = 7.2 Hz, aromatic H, 2H), 7.61 (d, *J* = 7.2 Hz, aromatic H, 2H), 7.41 (t, *J* = 7.2 Hz, aromatic H, 2H), 7.32 (t, *J* = 7.2 Hz, aromatic H, 2H), 7.04 (d, *J* = 7.2 Hz, N*H*-, 1H), 5.41 (s, C*H*-, 1H), 5.05-5.02 (m, C*H*-, 1H), 4.44-4.40 (m, CH_2-, 2H), 4.24-4.22 (m, C*H*-, 1H), 3.75 (bs, PEG CH_2-, 2H), 3.63 (bs, PEG CH_2-, 4H), 3.57-3.56 (m, PEG CH_2-, 2H), 3.99-3.37 (m, CH_2-, 2H), 3.28 (t, *J* = 6.6 Hz, CH_2-, 2H), 2,79 (s, NHS-CH_2-, 4H), 2.53 (s, CH_2-, 2H), 2.03-

2.00 (m, CH_2-, 1H), 1.88-1.84 (m, CH_2-, 1H), 1.67-1.61 (m, CH_2-, 2H,), 1.57-1.53 (m, CH_2-, 2H); ^{13}C NMR (126 MHz, $CDCl_3$): δ 171.42, 168.59, 168.10, 162.66, 156.53, 143.93, 141.27, 127.67, 127.01, 125.03, 119.95, 70.30, 70.0, 66.93, 66.56, 51.0, 49.91, 47.23, 40.72, 36.54, 36.50, 32.05, 28.23, 25.52, 25.38, 22.14; HRMS (ESI): m/z $[M+Na]^+$ calcd for $C_{32}H_{38}N_6O_9Na$: 673.2592, found: 673.2591.

Synthesis of compound 22. Compound **2** (20.0 mg, 37.7 μmol) and linker **21** (27.0 mg, 41.56 μmol) were dissolved in anhydrous DMF (300 μL) and to this solution DIPEA (~7.3 μL, 56.68 μmol) was added to adjust pH at ~8.5. The reaction mixture was stirred for 6 h at room temperature under anhydrous conditions. The solvent was removed and the crude reaction mixture was dried and treated with a 20% solution of piperidine-DMF (1 mL, 2:8) for 1 h. Solvent was removed under vacuum and the crude product was purified by semi-preparative RP-HPLC to afford compound **22** (23.8 mg, 74%) as colorless solid after lyophilization. Analytical RP-HPLC t_R = 16.2 min (gradient 5 to 100% B in 30 min); ^{1}H NMR (600 MHz, D_2O): δ 4.42 (d, *J* = 7.8 Hz, 1H), 4.39 (d, *J* = 7.8 Hz, 1H), 4.21 (dd, *J* = 8.4, 6.0 Hz, 1H), 3.92 (dd, *J* = 12.6, 2.4 Hz, 1H), 3.87-3.85 (m, 2H), 3.76-3.73 (m, 2H), 3.71-3.69 (m, 4H), 3.68-3.65 (m, 2H), 3.64 (bs, 4H), 3.62-3.58 (m, 4H), 3.54-3.52 (m, 1H), 3.49 (q, *J* = 7.8 Hz, 1H), 3.43-3.39 (m, 1H), 3.34-3.30 (m, 1H), 3.29-3.27 (m, 2H), 3.26-3.23 (m, 1H), 3.15 (t, *J* = 5.4 Hz, 2H), 2.65 (td, *J* = 6.6, 1.8 Hz, 2H), 2.56-2.51 (m, 4H), 1.79-1.73 (m, 1H), 1.71-1.65 (m, 1H), 1.60-1.50 (m, 6H), 1.43-1.36 (m, 2H), 1.33-1.25 (m, 8H); ^{13}C NMR (126 MHz, D_2O): δ 175.02, 174.93, 103.92, 103.01, 79.43, 76.34, 75.74, 75.46, 73.84, 73.52, 71.94, 71.70, 70.53 (2C's), 69.53, 67.62, 62.0, 61.11, 54.94, 51.87, 40.14, 39.61, 36.56, 32.10, 31.71, 31.38, 29.69 (2C's), 29.29, 29.12, 28.81, 28.56, 25.95, 23.36; HRMS (ESI): m/z [M+H]+ calcd for C35H67N6O15S: 843.4380, found: 843.4378; m/z $[M+Na]^+$ calcd for $C_{35}H_{67}N_6O_{15}SNa$: 865.4199, found: 865.4209.

Synthesis of conjugate 23. Conjugate **23** was obtained on treatment of compound **22** (5.41 mg, 6.42 μmol) with NHS-activated PEG **7** (12 mg, 1.07 μmol) in anhydrous DMF (150 μL) at room temperature under an argon atmosphere followed by the procedure described for conjugate **9**. The reaction mixture was incubated for ~3 h at room temperature and an additional ~21 h at 37 ºC. After ~24 h, the solvent was removed and the resulting crude reaction mixture was purified by C_{18} Sep-pak chromatography using gradient elution 0.1 % aq. AcOH to 8:2 MeOH/H_2O to afford tetravalent lactose conjugate **23** (13.8 mg, 91%) as a white amorphous power after lyophilization. Substitution of the PEG scaffold was determined by ^{1}H NMR integration of the underlined peaks to be lactose:PEG = 4:4. ^{1}H NMR (600 MHz, D_2O): 4.43 (d, *J* = 7.8 Hz, 1H), 4.40 (d, *J* = 7.8 Hz, 1H), 4.22 (dd, *J* = 8.4, 6.0 Hz, 1H), 3.93 (dd, *J* = 10.8, 1.8 Hz, 1H), 3.88-3.86 (m, 2H), 3.78-3.68 (m, 6H), 3.66 (band, PEG C*H*$_2$, 254), 3.63-3.60 (m, 8H), 3.59-3.53 (m, 4H), 3.50 (dd, *J* = 9.6, 7.8 Hz, 1H), 3.46 (s, 2H), 3.43-3.39 (m, 1H), 3.35-3.25 (m, 7H), 2.66 (t, *J* = 6.6 Hz, 2H), 2.54 (t, *J* = 6.6 Hz, 4H), 2.50 (bs, PEG-COC*H*$_2$C*H*$_2$CO-, 4H), 1.80-1.75 (m, 1H), 1.72-1.65 (m, 1H), 1.61-1.51 (m, 6H), 1.44-1.37 (m, 2H), 1.33-1.28 (m, 8H); ^{13}C NMR (126 MHz, D_2O): δ 175.68 (2C's), 175.00, 174.93, 103.92, 103.03, 79.43, 76.34, 75.74, 75.47, 73.85, 75.53, 71.95, 71.68, 71.57, 70.58 (PEG *C*H$_2$-), 70.41 (2C's), 69.86, 69.84, 69.54, 67.65, 62.0, 61.12, 54.92, 51.87 (2C's), 39.95 (2C's), 39.65, 36.70, 32.13, 32.07 (2C's), 31.74, 31.40, 29.73, 29.35, 29.18, 28.87, 28.59, 25.99, 23.39; The MALDI-TOF spectrum showed the average mass centered at 14.0 kDa and expected average mass was 14.1 kDa.

Synthesis of compound 24. Compound **24** was obtained by coupling compound **5** (12 mg, 13.0 μmol) and linker **21** (9.3 mg, 14.3 μmol), by following the procedure for compound **22** in a 75% yield (11.2 mg), as an amorphous powder after semi-preparative RP-HPLC purification and lyophilization. Analytical RP-HPLC t_R = 24.9 min (gradient 5 to 100% B in

30 min); ^{1}H NMR (600 MHz, D_2O): δ 5.24 (d, *J* = 4.2 Hz, 1H), 5.12 (d, *J* = 2.4 Hz, 1H), 4.54 (d, *J* = 7.8 Hz, 1H), 4.47 (d, *J* = 8.4 Hz, 1H), 4.27 (q, *J* = 6.6 Hz, 1H), 4.21 (dd, *J* = 8.4, 6.0, 1H), 4.19 (q, *J* = 3.6, 1H), 4.17-4.15 (m, 1H), 3.95-3.92 (m, 2H), 3.86-3.83 (m, 2H), 3.77 (dd, *J* = 3.0, 11.4 Hz, 1H), 3.75-3.70 (m, 10H), 3.69-3.66 (m, 3H), 3.65 (band, PEG C*H*$_2$, 4H), 3.62-3.60 (m, 2H), 3.54-3.50 (m, 2H), 3.44-3.39 (m, 1H), 3.38-3.36 (m, 1H), 3.33 (t, *J* = 6.0 Hz, 1H), 3.31-3.28 (m, 3H), 3.16 (t, *J* = 5.4 Hz, 2H), 2.65 (td, *J* = 1.8, 6.6 Hz, 2H), 2.65-2.52 (m, 4H), 1.99 (s, 6H), 1.78-1.73 (m, 1H), 1.71-1.66 (m, 1H), 1.60-1.48 (m, 7H), 1.43-1.36 (m, 2H), 1.33-1.31 (m, 2H), 1.25 (bs, 6H), 1.19 (d, *J* = 6.6 Hz, 3H); ^{13}C NMR (126 MHz, D_2O): δ 175.79, 175. 31, 175.01, 174.91, 102.10, 101.05, 99.62, 92.30, 77.22, 76.66, 76.33, 76.14, 73.39, 72.68, 72.06, 71.60, 70.94, 70.52 (PEG *C*H_2-), 69.47, 68.77, 68.65, 67.82, 67.60, 67.60, 67.36, 64.02, 62.29, 62.16, 61.18, 56.40, 54.95, 51.86, 50.49, 40.09, 39.60, 36.54, 32.08, 31.70, 31.37, 29.70, 29.52, 29.27, 28.98, 28.84, 28.55, 26.02, 23.35, 23.26, 22.92, 16.14; HRMS (ESI): m/z $[M+H]^+$ calcd for $C_{51}H_{93}N_8O_{24}SH$: 1233.6018, found: 1233.6023.

Synthesis of compound 25. Compound **25** was obtained by coupling compound **6** (12 mg, 13.6 μmol) with linker **21** (9.7 mg, 15.0 μmol) following the procedure for compound **22** in a 74 % yield (12.1 mg), as an amorphous colorless powder after semi-preparative RP-HPLC purification and lyophilization. Analytical RP-HPLC t_R = 25.0 min (gradient 5 to 100% B in 30 min); ^{1}H NMR (600 MHz, D_2O): δ 5.27 (d, *J* = 6.0 Hz, 1H), 5.19 (d, *J* = 3.4 Hz, 1H), 4.56 (d, *J* = 10.8 Hz, 1H), 4.44 (d, *J* = 12.0 Hz, 1H), 4.27-4.19 (m, 3H), 4.15 (td, *J* = 8.4, 1.2 Hz, 1H), 3.96-3.92 (m, 3H), 3.89-3.86 (m, 1H), 3.84 (bs, 2H), 3.76-3.67 (m, 12H), 3.65 (band, PEG C*H*$_2$-, 4H), 3.62-3.58 (m, 1H), 3.54-3.50 (m, 2H), 3.45-3.42 (m, 1H), 3.40-3.32 (m, 2H), 3.31-3.27 (m, 3H), 3.16 (t, *J* = 7.8 Hz, 2H), 2.65 (td, *J* = 1.2, 9.6 Hz, 2H), 2.56-2.52 (m, 4H), 1.99 (s, 3H), 1.78-1.67 (m, 4H), 1.61-1.49 (m, 7H), 1.43-1.39 (m, 2H), 1.36-1.31 (m,

2H), 1.25 (bs, 5H), 1.18 (d, *J* = 9.6 Hz, 3H); ^{13}C NMR (126 MHz, D_2O): δ 175.31, 175. 01, 174.92, 102.12, 101.10, 99.76, 94.03, 77.20, 76.31, 75.92, 73.53, 73.40, 72.13, 71.61, 70.98, 70.51, 70.52 (PEG *C*H_2-), 70.51, 70.25, 69.03, 68.67, 67.71, 67.61, 67.36, 64.49, 62.25, 62.12, 60.66, 56.36, 54.95, 51.89, 40.10, 39.60, 36.55, 32.09, 31.70, 31.37, 29.70, 29.52, 29.27, 29.22, 28.84, 28.55, 26.02, 23.35, 23.26, 16.14; HRMS (ESI): m/z [M+H]+ calcd for C49H90N7O24SH: 1192.5752, found: 1192.5763; m/z $[M+Na]^+$ calcd for $C_{49}H_{90}N_7O_{24}SNa$: 1214.5572, found: 1214.5566.

Synthesis of conjugate 26. Conjugate **26** was obtained on treatment of compound **24** (5.5 mg, 4.46 μmol) with NHS-activated PEG **7** (10 mg, 0.89 μmol, 1 equiv) following the procedure for conjugate **23**. Yield: (12.55 mg, 90%); Substitution of the PEG scaffold was determined by ^{1}H NMR integration of the underlined peaks to be A-type II:PEG = 4:4. ^{1}H NMR (600 MHz, D_2O): <u>5.30</u> (d, *J* = 4.2 Hz, 1H), <u>5.13</u> (d, *J* = 4.2 Hz, 1H), 4.55 (d, *J* = 7.8 Hz, 1H), 4.45 (d, *J* = 8.4 Hz, 1H), 4.27 (q, *J* = 6.6 Hz, 1H), 4.23-4.20 (m, 2H), 4.18-4.16 (m, 2H), 3.95 (t, *J* = 3.6 Hz, 2H), 3.93-3.92 (m, 1H), 3.87-3.84 (m, 3H), 3.79-3.77 (m, 3H), 3.76-3.73 (m, 7H), 3.71-3.68 (m, 2H), 3.66 (band, PEG C*H*$_2$-, 243H), 3.62 (band, PEG C*H*$_2$-, 10H), 3.59-3.55 (m, 6H), 3.54-3.52 (m, 2H), 3.45 (bs, 2H), 3.42-3.38 (m, 2H), 3.35-3.32 (m, 4H), 3.30-3.28 (m, 4H), 2.65 (t, *J* = 7.2 Hz, 2H), 2.56-2.52 (m, 4H), <u>2.49</u> (s, PEG-COC*H*$_2$C*H*$_2$CO-, 4H), 1.99 (s, 6H), 1.80-1.75 (m, 1H), 1.70-1.66 (m, 1H), 1.59-1.50 (m, 7H), 1.42-1.38 (m, 2H), 1.35-1.30 (m, 2H), 1.26 (bs, 6H), 1.20 (d, *J* = 6.6 Hz, 3H); ^{13}C NMR (126 MHz, D_2O): δ 175.77, 175.68 (2C's), 175.25, 175.00, 174.94, 102.09, 101.05, 99.62, 92.31, 77.25, 76.66, 76.34, 76.14, 73.39, 72.69, 72.06, 71.59, 70.94, 70.58 (PEG C*H*$_2$-), 70.41, 69.85, 69.84, 69.47, 68.78, 68.66, 67.83, 67.64, 64.02, 62.29, 62.15, 61.21, 56.42, 54.93, 51.87 (2C's), 50.50, 46.05, 39.93, 39.94 (2C's), 39.64, 36.70, 32.12, 32.07 (2C's), 31.73, 31.39, 29.74, 29.55, 29.32, 29.27, 28.89, 28.59, 26.05, 23.38, 23.27, 22.93, 16.16; The

MALDI-TOF spectrum showed the average mass centered at 15.1 kDa and expected average value was 15.6 kDa.

Synthesis of conjugate 27. Conjugate **27** was obtained on treatment of compound **25** (5.32 mg, 4.46 μmol) with NHS-activated PEG **7** (10 mg, 0.89 μmol, 1 equiv) following the procedure for conjugate **23**. Yield: (12.65 mg, 91%); Substitution of the PEG scaffold was determined by ^{1}H NMR integration of the underlined peaks to be B-type II:PEG = 4:4. ^{1}H NMR (600 MHz, D_2O): δ 5.28 (d, *J* = 3.6 Hz, 1H), 5.19 (d, *J* = 3.6 Hz, 1H), 4.57 (d, *J* = 7.8 Hz, 1H), 4.50 (d, *J* = 7.8 Hz, 1H), 4.27-4.21 (m, 3H), 4.15 (t, *J* = 6.0 Hz, 1H), 3.96-3.92 (m, 3H), 3.89-3.82 (m, 4H), 3.77-3.70 (m, 4H), 3.68-3.61 (band, PEG C*H*$_2$-, 268H), 3.59-3.54 (m, 2H), 3.54-3.51 (m, 1H), 3.46 (m, 2H), 3.44-3.39 (m, 1H), 3.37-3.32 (m, 3H), 3.31-3.28 (m, 3H), 2.65 (t, *J* = 6.6 Hz, 2H), 2.55-2.51 (m, 4H), 2.49 (s, PEG-COC*H*$_2$C*H*$_2$CO-, 4H), 1.99 (s, 3H), 1.81-1.75 (m, 2H), 1.71-1.68 (m 2H), 1.58 (t, *J* = 7.2 Hz, 2H), 1.56-1.50 (m, 5H), 1.44-1.38 (m, 2H), 1.35-1.31 (m, 2H), 1.26 (bs, 5H), 1.19 (d, *J* = 6.0 Hz, 3H); ^{13}C NMR (126 MHz, D_2O): δ 175.68 (2C's), 175.24, 175.00, 174.93, 102.12, 101.11, 99.76, 94.03, 77.24, 77.20, 76.32, 76.14, 75.92, 73.52, 73.40, 72.69, 72.13, 71.57, 70.99, 70.58 (PEG C*H*$_2$-), 70.41, 70.25, 69.86, 69.84, 69.04, 68.68, 68.77, 67.65, 64.49, 62.25, 62.11, 61.21, 56.37, 54.93, 49.85, 46.05, 39.93, 39.94 (2C's), 39.64, 36.70, 32.12, 32.07 (2C's), 31.74, 31.39, 29.75, 29.56, 29.33, 29.28, 28.89, 28.59, 26.05, 23.39, 23.28, 16.16; The MALDI-TOF spectrum showed the average mass centered at 15.4 kDa and expected average value was 15.5 kDa.

Synthesis of conjugate 31. Conjugate **31** was obtained by coupling compound **23** (10 mg, 0.70 μmol) and propargyl sialoside **28** (0.40 mg, 1.13 μmol) following the general procedure for CuAAC ligation, in a 79% yield (9.5 mg) as white foam after C_{18} Sep-pak chromatography purification using eluent system H_2O to MeOH/H_2O (8:2) and

lyophilization. Substitution of the PEG scaffold was determined by ^{1}H NMR integration of the underlined peaks to be lactose:Neu5Ac:PEG = 4:4:1. ^{1}H NMR (600 MHz, D_2O): δ 7.98 (s, 1H), 4.89 (d, *J* = 12.0 Hz, 1H), 4.43-4.92 (m, 3H), 4.18 (t, *J* = 7.2 Hz, 1H), 3.92 (dd, *J* = 10.8, 1.8 Hz, 1H), 3.88-3.82 (m, 4H), 3.78-3.78 (m, 6H), 3.75-3.71 (m, 4H), 3.66 (band, PEG C*H*$_2$, 252H), 3.62-3.60 (m, 10H), 3.59-3.53 (m, 8H), 3.50 (dd, *J* = 9.6, 7.8 Hz, 1H), 3.45 (s, 2H), 3.40-3.36 (m, 1H), 3.35-3.31 (m, 4H), 3.30-3.24 (m, 2H), 2.68 (dd, *J* = 13.2, 4.8 Hz, 1H), 2.60-2.57 (m, 2H), 2.51-2.50 (m, 4H), 2.49 (s, PEG-COC*H*$_2$C*H*$_2$CO-, 4H), 1.99 (s, 3H), 1.90-1.87 (m, 2H), 1.79 (t, *J* = 5.4 Hz, 1H), 1.78-1.72 (m, 1H), 1.71-1.64 (m, 1H), 1.56 (t, *J* = 7.2 Hz, 2H), 1.51 (t, *J* = 7.2 Hz, 2H), 1.30-1.26 (m, 11H); ^{13}C NMR (126 MHz, D_2O): δ 175.52 (2C's), 174.76, 174.53, 170.66, 144.22, 125.94, 103.76, 102.87, 99.57, 79.24, 76.18, 75.58, 75.31, 73.85, 73.69, 73.36, 71.78, 71.51, 71.40, 70.42 (PEG *C*H$_2$-), 70.24, 69.68 (2C's), 69.37, 69.09, 67.90, 67.45, 63.96, 61.85, 60.95, 58.13, 54.61, 54.21, 52.57, 50.94, 40.27, 39.77 (2C's), 39.76, 39.41 (2C's), 36.47, 31.89, 31.88, 31.34, 31.19, 29.68, 29.57 (2C's), 29.20, 29.03, 28.71, 25.83, 22.92, 22.70; The MALDI-TOF spectrum showed the average mass centered at 15.2 kDa and expected average value was 15.5 kDa.

Synthesis of conjugate 32. Conjugate **32** was obtained through coupling of compound **23** (9 mg, 0.64 μmol) with propargyl 3'-sialyllactose **29** (2.64 mg, 3.85 μmol) following the general procedure for CuAAC ligation, in 84% yield (9.1 mg) as white powder after C_{18} Sep-pak chromatography purification using solvent gradient H_2O to MeOH/H_2O (8:2) and lyophilization. Substitution of the PEG scaffold was determined by ^{1}H NMR integration of the underlined peaks to be lactose:3'-sialyllactose:PEG = 4:4:1. ^{1}H NMR (600 MHz, D_2O): δ 8.03 (s, 1H), 4.95 (d, *J* = 12.0 Hz, 1H), 4.82 (d, *J* = 12.6 Hz, 1H), 4.53 (d, *J* = 7.8 Hz, 1H), 4.48 (d, *J* = 7.8 Hz, 1H), 4.31-4.40 (m, 4H), 4.18 (t, *J* = 6.6 Hz, 1H), 4.06 (dd, *J* = 10.2, 3.0 Hz, 1H), 3.94-3.91 (m, 2H), 3.88-3.83 (m, 2H), 3.82-3.76 (m, 4H), 3.75-3.71 (m, 4H), 3.66-

3.59 (band, PEG CH_2-, 277H), 3.57-3.48 (m, 4H), 3.45 (s, 2H), 3.41-3.36 (m,1H), 3.34-3.31 (m, 6H), 2.72 (dd, J = 12.0, 4.8 Hz, 1H), 2.61-2.57 (m, 2H), 2.53-2.51 (m, 4H), 2.49 (s, PEG-COCH_2CH_2CO-, 4H), 1.98 (s, 3H), 1.89 (t, J = 12.0 Hz, 2H), 1.75 (t, J = 12.0 Hz, 1H), 1.71-1.64 (m, 2H), 1.56 (t, J = 7.2 Hz, 2H), 1.51(t, J = 7.2 Hz, 2H), 1.30-1.26 (m, 11H); ^{13}C NMR (126 MHz, D_2O): δ 175.87, 175.56 (2C's), 174.80, 174.68, 174.60, 144.22, 126.12, 103.80, 103.53, 102.90, 102.27, 100.74, 79.30, 79.11, 76.36, 76.21, 76.03, 75.69, 75.61, 75.34, 75.21, 73.75, 73.72, 73.58, 73.40, 72.61, 71.82, 71.54, 71.44, 70.53 (PEG CH$_2$-), 70.44, 70.27 (2C's), 69.70 (2C's), 69.41, 69.19, 68.96, 68.33, 67.49, 63.45, 62.91, 61.87 (2C's), 60.99, 60.98, 54.63, 52.56, 50.98, 49.72, 45.92, 40.50, 39.80 (2C's), 39.46, 36.51, 31.94, 31.93 (2C's), 31.37, 31.25, 29.69, 29.59 (2C's), 29.22, 29.04, 28.73, 25.85, 22.89, 22.77; The MALDI-TOF spectrum showed the average mass centered at 16.0 kDa and expected average value was 16.7 kDa.

Synthesis of conjugate 33. Conjugate **33** was also obtained through coupling of compound **23** (9 mg, 0.638 μmol) with propargyl 6'-linked sialolactose **30** (2.56 mg, 3.82 μmol) by following the general procedure for CuAAC ligation, in 85% yield (9.12 mg) as white powder after C_{18} Sep-pak chromatography purification using solvent gradient H_2O to MeOH/H_2O (7:3) and lyophilization. Substitution of the PEG scaffold was determined by ^{1}H NMR integration of the underlined peaks to be lactose:6'-sialyllactose:PEG = 4:4:1. ^{1}H NMR (600 MHz, D_2O): δ 8.03 (s, 1H), 4.95 (d, J = 12.6 Hz, 1H), 4.83 (d, J = 12.6 Hz, 1H), 4.54 (d, J = 7.8 Hz, 1H), 4.41-4.37 (m, 4H), 4.18 (t, J = 6.6 Hz, 1H), 3.93-3.88 (m, 4H), 3.84-3.79 (m, 4H), 3.77-3.71 (m, 8H), 3.66-3.47 (band, PEG CH_2-, 272H), 3.45 (s, 2H), 3.41-3.36 (m, 1H), 3.33-3.30 (m, 8H), 2.65 (dd, J = 12.0, 4.8 Hz, 1H), 2.60 (t, J = 6.6 Hz, 2H), 2.52-2.51 (m, 4H), 2.49 (s, PEG-COCH_2CH_2CO-, 4H), 1.98 (s, 3H), 1.90 (t, J = 6.6 Hz, 2H), 1.81-1.74 (m, 1H), 1.68 (t, J = 12.0 Hz, 2H), 1.56 (t, J = 6.6 Hz, 2H), 1.51(t, J = 6.6 Hz, 2H), 1.30-1.26

(m, 11H); ^{13}C NMR (126 MHz, D_2O): δ 175.85, 175.66 (2C's), 174.90, 174.68, 174.71, 174.39, 126.24, 104.22, 103.91, 103.02, 102.29, 101.30, 80.56, 79.41, 76.32, 75.73, 75.67, 75.61, 75.46, 74.67, 73.84, 73.62, 73.51, 73.35, 72.76, 71.94, 71.77, 71.66, 71.55, 70.56, (PEG *C*H_2-), 70.39, 69.82, 69.53, 69.48, 69.36, 69.32, 67.61, 63.51, 63.62, 63.05, 61.99, 61.25, 61.11, 54.75, 52.78, 51.10, 49.84, 41.10, 39.93 (2C's), 39.59, 36.63, 32.05 (2C's), 31.50, 31.36, 31.20 (2C's), 29.82, 29.72, 29.35, 29.17, 28.86, 29.04, 25.98, 23.04, 22.90; The MALDI-TOF spectrum showed the average mass centered at 16.0 kDa and expected average value was 16.7 kDa.

Synthesis of conjugate 34. Conjugate **34** was obtained by coupling compound **26** (10 mg, 0.70 μmol) and propargyl sialoside **28** (0.40 mg, 1.13 μmol) following the general procedure for CuAAC ligation, in a 79% yield (9.5 mg) as white foam after C_{18} chromatography purification using eluent gradient H_2O to MeOH/H_2O (8:2) and lyophilization. Substitution of the PEG scaffold was determined by ^{1}H NMR integration of the underlined peaks to be A-type II:Neu5Ac:PEG = 4:4:1. ^{1}H NMR (600 MHz, D_2O): δ 7.98 (s, 1H), 5.28 (d, *J* = 4.2 Hz, 1H), 5.20 (d, *J* = 2.4 Hz, 1H), 4.89 (d, *J* = 12.6 Hz, 1H), 4.57 (d, *J* = 7.8 Hz, 1H), 4.44 (d, *J* = 7.8 Hz, 1H), 4.40 (t, *J* = 6.6 Hz, 2H), 4.26-4.25 (m, 1H), 4.23 (d, *J* = 1.8 Hz, 1H), 4.19-4.14 (m, 2H), 3.96-3.92 (m, 3H), 3.89-3.82 (m, 4H), 3.78-3.76 (m, 2H), 3.75-3.70 (m, 4H), 3.66 (band, PEG C*H*$_2$-, 269H), 3.62-3.60 (band, PEG C*H*$_2$-, 4H), 3.57 (t, *J* = 5.4 Hz, 2H), 3.55-3.53 (m, 2H), 3.46 (bs, 2H), 3.40-3.38 (m, 2H), 3.33 (q, *J* = 5.4 Hz, 2H), 2.67 (dd, *J* = 12.6, 4.2 Hz, 1H), 2.59 (t, *J* = 6.6 Hz, 2H), 2.52-2.50 (m, 4H), 2.49 (m, PEG-COC*H*$_2$C*H*$_2$CO-, 4H), 2.0 (s, 3H), 1.98 (s, 3H), 1.89-1.86 (m, 3H), 1.79 (t, *J* = 12.6 Hz, 1H), 1.76-1.72 (m, 2H), 1.70-1.65 (m, 2H), 1.52-1.48 (m, 8H), 1.30-1.28 (m, 2H), 1.23 (bs, 7H), 1.18 (d, *J* = 6.6 Hz, 3H); ^{13}C NMR (126 MHz, D_2O): δ 175.96, 175.68, 175.67 (2C's), 175.22, 174.89, 174.66, 170.81, 126.12, 102.12, 101.10, 99.74 (2C's), 94.03, 77.20, 76.32, 75.92, 74.02, 73.52, 73.40,

72.69, 72.13, 71.56, 70.98, 70.57 (PEG C*H*$_2$-), 70.40, 70.25, 69.83 (2C's), 69.26, 69.04, 68.68, 68.05, 67.76, 67.61, 64.49, 64.12, 62.24, 62.11, 61.20, 58.29, 56.36, 54.76, 54.37, 52.74, 51.11, 49.85, 46.05, 40.43, 39.93 (2C's), 39.57, 36.64, 32.06 (2C's), 31.50, 31.40, 29.84, 29.74, 29.55, 29.34, 28.28, 28.90, 26.05, 23.28, 23.08, 22.86, 16.16; The MALDI-TOF spectrum showed the average mass centered at 17.0 kDa and expected average value was 17.0 kDa.

Synthesis of conjugate 35. Conjugate **35** was obtained by coupling compound **26** (8.0 mg, 0.51 μmol) and propargyl 3'-sialolactose **29** (2.06 mg, 3.07 μmol) following the general procedure for CuAAC ligation, in 86% yield (8.11 mg) as white powder after C_{18} Sep-pak chromatography purification using gradient eluent H_2O to MeOH/H_2O (8:2) and lyophilization. Substitution of the PEG scaffold was determined by ^{1}H NMR integration of the underlined peaks to be A-type II:3'-sialyllactose:PEG = 4:4:1.^{1}H NMR (600 MHz, D_2O): δ 8.03 (s, 1H), 5.30 (d, *J* = 3.0 Hz, 1H), 5.13 (d, *J* = 2.4 Hz, 1H), 4.94 (d, *J* = 12.6 Hz, 1H), 4.82 (d, *J* = 12.6 Hz, 1H), 4.55 (d, *J* = 7.8 Hz, 1H), 4.55 (d, *J* = 7.8 Hz, 1H), 4.48 (d, *J* = 8.4 Hz, 1H), 4.45 (d, *J* = 8.4 Hz, 1H), 4.41 (t, *J* = 6.0 Hz, 2H), 4.27 (d, *J* = 6.6 Hz, 1H), 4.18(bs, 3H), 4.06 (dd, *J* = 7.8, 2.4 Hz, 1H), 3.95-3.91 (m, 4H), 3.86-3.81 (m, 4H), 3.80-3.75 (m, 6H), 3.72-3.71 (m, 10H), 3.66-3.60 (band, PEG C*H*$_2$-, 283H), 3.57-3.49 (m, 12H), 3.45 (bs, 2H), 3.40-3.37 (m, 2H), 3.33-3.27 (m, 4H), 2.71 (dd, *J* = 12.6, 4.8 Hz, 1H), 2.60-2.58 (m, 2H), 2.51-2.50 (m, 4H), 2.49 (s, PEG-COC*H*$_2$C*H*$_2$CO-, 4H), 1.98 (s, 9H), 1.90-1.88 (m, 2H), 1.75 (t, *J* = 12.6 H, 2H), 1.70-1.67 (m, 2H), 1.51-1.49 (m, 4H), 1.30-1.29 (m, 2H), 1.24 (bs, 7H), 1.18 (d, *J* = 6.0 Hz, 3H); ^{13}C NMR (126 MHz, D_2O): δ 175.97, 175.66 (2C's), 175.24, 174.90, 170.80, 174.70, 144.57, 126.21, 103.64, 102.38, 102.07, 101.04, 100.82, 99.61, 92.30, 79.22, 77.23, 76.65, 76.47, 76.33, 76.14, 75.81, 75.33, 73.86, 73.69, 73.38, 73.02, 72.73, 71.55, 72.11, 71.55, 70.56 (PEG *C*H$_2$-), 69.82 (2C's), 70.24, 69.46, 69.31, 69.08,

68.67, 68.76, 68.65, 68.44, 67.82, 67.60, 64.02, 63.57, 63.45 (2C's), 63.02, 62.27, 62.14, 61.99. 61.19, 61.05, 56.41, 54.75, 52.68, 51.09, 50.48, 46.63, 39.92 (2C's), 39.58, 36.63, 32.05 (2C's), 31.48, 31.37, 29.82, 29.73, 29.53, 29.32, 29.27, 28.88, 26.03, 23.27, 23.02, 22.92, 16.15; The MALDI-TOF spectrum showed the average mass centered at 18.0 kDa and expected average value was 18.3 kDa.

Synthesis of conjugate 36. Conjugate **36** was obtained by coupling compound **26** (8.0 mg, 0.51 μmol) and propargyl 6'-sialolactose **30** (2.0 mg, 3.07 μmol) following the general procedure for CuAAC ligation, in 84% yield (7.9 mg) as white foam after C_{18} Sep-pak chromatography purification using MeOH/H_2O (8:2) and lyophilization. Substitution of the PEG scaffold was determined by ^{1}H NMR integration of the underlined peaks to be A-type II:6'sialyllactose:PEG = 4:4:1.^{1}H NMR (600 MHz, D_2O): δ 8.03 (s, 1H), 5.30 (d, J = 2.8 Hz, 1H), 5.13 (d, J = 2.4 Hz, 1H), 4.95 (d, J = 12.6 Hz, 1H), 4.83 (d, J = 12.6 Hz, 1H), 4.59 (t, J = 7.2 Hz, 2H), 4.45 (d, J = 8.4 Hz, 1H), 4.41(t, J = 6.6 Hz, 2H), 4.38 (d, J = 7.8 Hz, 1H), 4.27 (dd, J = 13.2, 6.0 Hz, 1H), 4.20-4.16 (m, 4H), 3.95-3.90 (m, 4H), 3.89-3.81 (m, 8H), 3.79-3.70 (m, 18H), 3.66-3.60 (band, PEG CH_2-, 272H), 3.59-3.50 (m, 12H), 3.45 (bs, 2H), 3.39-3.36 (m, 2H), 3.34-3.32 (m, 4H), 3.30 (band, PEG CH_2-, 4H), 2.66 (dd, J = 12.6, 4.8 Hz, 1H), 2.60 (t, J = 7.2 Hz, 2H), 2.52-2.50 (m, 4H), 2.49 (s, PEG-COCH_2CH_2CO-, 4H), 1.99 (s, 6H), 1.98 (s, 3H), 1.91-1.88 (m, 2H), 1.80-1.71 (m, 2H), 1.68 (m, 2H), 1.76-1.71 (m, 1H), 1.52-1.49 (m, 4H), 1.30-1.29 (m, 2H), 1.24 (bs, 7H), 1.19 (d, J = 6.6 Hz, 3H); ^{13}C NMR (126 MHz, D_2O): ö 175.85, 175.76, 175.67 (2C's), 175.24, 174.90, 174.72, 174.41, 144.56, 126.22, 14.21, 102.28, 102.08, 101.27, 101.04, 99.61, 92.30, 80.56, 77.23, 76.66, 76.33, 76.13, 75.67, 74.67, 73.62, 73.51, 73.38, 72.76, 72.68, 72.05, 71.77, 71.55, 70.92, 70.56 (PEG CH$_2$-), 70.39, 69.83, 69.47, 69.33, 68.77, 68.65, 67.82, 67.61, 64.51, 64.02, 63.63, 63.05, 62.28, 62.15, 61.24, 56.41, 54.76, 52.78, 51.09, 50.48, 49.84(2C's), 40.10, 39.92

(2C's), 39.59, 36.63, 32.06 (2C's), 31.49, 31.33, 29.82, 29.73, 29.53, 29.32, 29.27, 28.89, 26.03, 23.27, 23.04, 22.92, 16.15; The MALDI-TOF spectrum showed the average mass centered at 18.1 kDa and expected average value was 18.3 kDa

Synthesis of conjugate 37. Conjugate **37** was obtained by coupling compound **27** (10 mg, 0.70 μmol) and propargyl sialoside **28** (0.40 mg, 1.13 μmol), following the general procedure for CuAAC ligation, in 78% yield (9.3 mg) as a colorless powder after C_{18} Sep-pak chromatography purification using eluent gradient H_2O to MeOH/H_2O (8:2) and lyophilization. Substitution of the PEG scaffold was determined by ^{1}H NMR integration of the underlined peaks to be B-type II:Neu5Ac:PEG = 4:4:1.^{1}H NMR (600 MHz, D_2O): δ 7.98 (s, 1H), 5.30 (d, *J* = 3.6 Hz, 1H), 5.13 (d, *J* = 3.0 Hz, 1H), 4.89 (d, *J* = 12.6 Hz, 1H), 4.55 (d, *J* = 7.8 Hz, 1H), 4.45 (d, *J* = 8.4 Hz, 1H), 4.41 (t, *J* = 6.0 Hz, 2H), 4.27 (d, *J* = 6.6 Hz, 1H), 4.20-4.18 (m, 3H), 3.95-3.92 (m, 2H), 3.86-3.82 (m, 4H), 3.78-3.60 (band, PEG C*H*$_2$-, 280H), 3.58-3.45 (m, 4H), 3.40 (s, 2H), 3.38-3.34 (m, 1H), 3.33-3.30 (m, 4H), 2.67 (dd, *J* = 12.6, 4.2 Hz, 1H), 2.59 (t, *J* = 6.6 Hz, 2H), 2.51-2.50 (m, 4H), 2.49 (m, PEG-COC*H*$_2$C*H*$_2$CO-, 4H), 2.02 (s, 3H), 1.99 (s, 3H), 1.98 (s, 3H), 1.89-1.87 (m, 2H), 1.77 (t, *J* = 12.6 Hz, 1H), 1.76-1.71 (m, 1H), 1.70-1.65 (m, 2H), 1.52-1.48 (m, 6H), 1.29-1.28 (m, 2H), 1.23 (bs, 7H), 1.18 (d, *J* = 6.6 Hz, 3H); ^{13}C NMR (126 MHz, D_2O): δ 175.95, 175.77, 175.66 (2C's), 175.22, 174.89, 174.66, 170.80, 126.17, 102.09, 101.05, 99.74, 99.62, 92.31, 77.25, 76.67, 76.34, 76.14, 74.02, 73.39, 72.69, 72.06, 71.55, 70.93, 70.57 (PEG *C*H$_2$-), 69.84, 69.47, 69.26, 68.77, 68.66, 68.05, 67.82, 67.61, 64.12, 64.02, 62.28, 62.15, 61.20, 58.30, 56.42, 54.76, 54.37, 52.74, 51.11, 50.50, 40.43, 39.93 (2C's), 39.57, 36.64, 32.06 (2C's), 31.50, 31.49, 29.84, 29.74, 29.56, 29.34, 28.91, 26.05, 23.28, 23.08, 22.93, 22.92, 16.16; The MALDI-TOF spectrum showed the average mass centered at 16.6 kDa and expected average value was 16.6 kDa.

Synthesis of conjugate 38. Conjugate **38** was obtained by coupling compound **27**(8.0 mg, 0.5 μmol) and propargyl 3'-linked sialolactose **29** (2.07 mg, 3.09 μmol), following the general procedure for CuAAC ligation, in 87% yield (8.11 mg) as white powder after C_{18} Sep-pak chromatography purification using eluent gradient H_2O to MeOH/H_2O (8:2) and lyophilization. Substitution of the PEG scaffold was determined by ^{1}H NMR integration of the underlined peaks to be B-type II:3'-sialyllatose:PEG = 4:4:1. ^{1}H NMR (600 MHz, D_2O): δ 8.02 (s, 1H), 5.28 (d, *J* = 4.2 Hz, 1H), 5.19 (d, *J* = 2.4 Hz, 1H), 4.95 (d, *J* = 12.6 Hz, 1H), 4.82 (d, *J* = 12.6 Hz, 1H), 4.57 (d, *J* = 7.8 Hz, 1H), 4.53 (d, *J* = 7.8 Hz, 1H), 4.48 (d, *J* = 7.8 Hz, 1H), 4.44 (d, *J* = 8.4 Hz, 1H), 4.41 (t, *J* = 6.6 Hz, 2H), 4.26 (d, *J* = 6.6 Hz, 1H), 4.23 (bs, 1H), 4.18-4.15 (m, 2H), 4.06 (dd, *J* = 10.2, 3.0 Hz, 1H), 3.94-3.91 (m, 4H), 3.89-3.83 (m, 4H), 3.82-3.77 (m, 4H), 3.75-3.70 (m, 4H), 3.66 (band, PEG C*H*$_2$-, 291H), 3.60 (bs, 4H), 3.58-3.53 (m, 8H), 3.45 (bs, 2H), 3.39-3.37 (m, 2H), 3.34-3.30 (m, 4H), 2.71 (dd, *J* = 12.6, 4.2 Hz, 1H), 2.60 (t, *J* = 6.6 Hz, 2H), 2.52-2.50 (m, 4H), 2.49 (s, PEG-COC*H*$_2$C*H*$_2$CO-, 4H), 1.98 (s, 6H), 1.89 (t, *J* = 7.2 Hz, 2H), 1.75 (t, *J* = 12.0 H, 2H), 1.69-1.64 (m, 2H), 1.52-1.49 (m, 4H), 1.31-1.28 (m, 2H), 1.24 (bs, 7H), 1.18 (d, *J* = 6.6 Hz, 3H); ^{13}C NMR (126 MHz, D_2O): δ 175.98, 175.67 (2C's), 175.23, 174.85, 174.83, 174.71, 144.52, 126.18, 103.64, 102.37, 102.10, 101.09, 100.78, 99.74, 94.01, 79.21, 77.19, 76.47, 76.30, 76.14, 75.90, 75.81, 75.33, 73.86, 73.70, 73.50, 73.39, 72.69, 72.11, 71.55 (2C's), 70.96, 72.05, 71.77, 70.56 (PEG *C*H$_2$-), 69.82 (2C's), 69.31, 69.05, 69.03, 68.67, 68.44, 67.75, 67.60, 64.48, 63.57, 63.01, 62.68, 62.23, 62.10, 61.99, 61.34, 61.19, 61.05, 56.36, 54.75, 52.68, 51.08, 50.48, 40.63, 39.92 (2C's), 39.58, 36.63, 32.05 (2C's), 31.85, 31.49, 31.34, 29.73, 29.53, 29.31, 29.27, 28.88, 26.03, 23.27, 23.01, 22.89, 21.48, 16.15, 14.21; The MALDI-TOF spectrum showed the average mass centered at 16.0 kDa and expected average value was 18.1 kDa.

Synthesis of conjugate 39. Conjugate **39** was obtained by coupling compound **27** (7.0 mg, 0.45 μmol) and propargyl 6'-sialolactose **30** (1.81 mg, 2.7 μmol) following the general procedure for CuAAC ligation, in 86% yield (7.11 mg) as white foam after C_{18} Sep-pak chromatography purification using eluent solvent H_2O to MeOH/H_2O (8:2) and lyophilization. Substitution of the PEG scaffold was determined by ^{1}H NMR integration of the underlined peaks to be B-type II:6'-sioalyllactose:PEG = 4:4:1. ^{1}H NMR (600 MHz, D_2O): δ 7.98 (s, 1H), 5.28 (d, *J* = 4.2 Hz, 1H), 5.19 (d, *J* = 2.4 Hz, 1H), 4.89 (d, *J* = 12.0 Hz, 1H), 4.57 (d, *J* = 7.8 Hz, 1H), 4.44 (d, *J* = 8.4 Hz, 1H), 4.40 (t, *J* = 6.0 Hz, 2H), 4.26 (d, *J* = 6.6 Hz, 1H), 4.24 (bs, 1H), 4.19-4.14 (m, 2H), 3.95-3.92 (m, 4H), 3.89-3.82 (m, 8H), 3.78-3.75 (m, 8H), 3.73-3.71 (m, 10H), 3.66 (band, PEG C*H*$_2$-, 281H), 3.60 (bs, 4H), 3.57-3.53 (m, 8H), 3.45 (bs, 2H), 3.39-3.37 (m, 2H), 3.34-3.30 (m, 4H), 2.67 (dd, *J* = 12.6, 4.8 Hz, 1H), 2.60-2.58 (m, 2H), 2.51-2.50 (m, 4H), 2.49 (s, PEG-COC*H*$_2$C*H*$_2$CO-, 4H), 2.0 (s, 3H), 1.98 (s, 3H), 1.89-1.87 (m, 2H), 1.77 (t, *J* = 12.6 H, 1H), 1.75-1.71 (m, 1H), 1.67-1.66 (m, 2H), 1.51-1.48 (m, 4H), 1.30-1.29 (m, 2H), 1.24 (bs, 7H), 1.18 (d, *J* = 6.6 Hz, 3H); ^{13}C NMR (126 MHz, D_2O): ö 175.95, 175.66 (2C's), 175.22, 174.88, 174.66, 170.80, 126.09, 102.11, 101.09, 99.82, 99.72, 94.02, 77.19, 76.31, 75.91, 74.00, 73.51, 73.39, 73.03, 72.68, 72.11, 71.55, 70.97, 72.05, 71.77, 70.56 (PEG *C*H$_2$-), 70.39 (2C's), 70.24, 69.82, 69.25, 69.03, 68.67, 68.05, 67.75, 67.60, 64.48, 64.11, 63.46 (2C's), 62.23, 62.10, 61.19, 58.29, 56.35, 54.75, 54.36, 52.73, 51.09, 50.48, 46.04, 40.42, 39.92 (2C's), 39.56, 36.63, 32.05 (2C's), 31.49, 31.34, 29.83, 29.73, 29.54, 29.32, 29.27, 28.89, 26.03, 23.27, 23.04, 22.86, 16.15; The MALDI-TOF spectrum showed the average mass centered at 16.8 kDa and expected average value was 18.1 kDa.

Fluorescence microscopy and clustering analysis on B cells. A-BCL **c**ells were prepared and grown as previously described.[22] Cells were grown in R10 media supplemented with

glutamax and 1% beta-mercaptoethanol added weekly in 12-well plates (Corning, Inc.). Plates were kept in a humidified incubator at 37 °C and 5% CO_2. For single-color fluorescence microscopy experiments, 2 x10^6 cells were washed and treated with 25 ng mL^{-1} of the indicated sample on ice for 1 h, then fixed using 1% PFA on ice for 20 min. Samples were treated with 1 μL mL^{-1} mouse anti-human IgM (clone IM260, Abcam) or mouse anti-human CD22 (clone HIB22, BD Pharmingen) at 4 °C overnight, washed, and stained with goat anti-mouse IgG (polyclonal, Sigma-Aldrich) conjugated with Alexa Flour 647 at room temperature for 1 hour. The loading of the fluorophores was approximately 2 dye per protein as determined by spectrophotometry. After washing, samples were transferred to 24-well plates (Corning, Inc.) with 12 mm circular cover glass slides pre-treated with 0.001% poly-L-lysine and spun at 300 x g for 15 minutes. Cover glass slides with samples were washed, mounted onto microscopy slides with Slowfade Antifade (Thermo Fisher), and sealed with Cytoseal 60. Samples were imaged on a laser scanning confocal microscope (Olympus IX81) at 60X. Ten cells from each condition were chosen for analysis based on transmitted and fluorescence images, in which each image was subjected to similar thresholding levels, and each cluster was analyzed using the particle analysis function on ImageJ.[106] The area of a single pixel in these images was 0.053 μm^2. The areas of each cluster from the analyses were plotted using beanplot in the R statistical package.[107] Analysis of the means and Student's t-test were performed in Graphpad Prism.

For co-localization studies, A-BCL cells were prepared as above, and 2 x 10^6 cells were washed and treated with either 0 ng mL^{-1} or 25 ng mL^{-1} of conjugate **36** on ice for one hour, and then fixed with 1% PFA on ice for 20 min. Cells were then treated with 1 μL mL^{-1} mouse anti-human CD22 (clone HIB22, BD Pharmingen) and 1 μL mL^{-1} rabbit anti-human

IgM (clone RM121, EMD Millipore) overnight at 4 °C. Samples were washed with PBS and stained with goat anti-mouse IgG (polyclonal, Sigma-Aldrich) conjugated with Alexa Fluor 647 and goat anti-rabbit IgG (polyclonal, Invitrogen) conjugated with Alexa Fluor 543 secondary antibodies for one hour at room temperature. Cells were washed with PBS and transferred to 12 mm circular coverslip slides pre-treated with 0.001% poly-L-lysine and spun at 300 x g for 15 minutes. Coverslip glass slides with samples were washed and mounted on microscopy slides with Slowfade Antifade (Thermo Fisher). Slides were imaged on spinning disk confocal microscope (Olympus IX-81) at 60X. Ten cells from each condition were chosen for analysis based on transmitted and fluorescence images. Background from each image was subtracted and the degree of co-localization was analyzed using coloc2 function on ImageJ. Results were plotted and analyzed using Prism software.

SUPPORTING INFORMATION

The Supporting Information is available free of charge on the ACS publications website at DOI: 10.1021/acs.bioconj-chem.xxxxx

Information including plots of receptor clustering data used for Table 1 and co-clustering analysis of Figure 3.

AUTHOR INFORMATION

Corresponding Author

*E-mail: ccairo@ualberta.ca

ORCID

Christopher W Cairo: 0000-0003-3363-8708

Todd L Lowary: 0000-0002-8331-8211

Lori J West: 0000-0002-1990-3651

Gour Chand Daskhan: 0000-0002-1805-5750

Notes

The authors report no competing financial interest.

ACKNOWLEDGEMENTS

This work was supported by the Alberta Glycomics Centre and the Natural Sciences and Engineering Research Council of Canada (NSERC).

References

(1) Varki, A., Cummings, R. D., Esko, J. D., Freeze, H. H., Stanley, P., Bertozzi, C. R., Hart, G. W., and Etzler, M. E. (2009), Cold Spring Harbor Laboratory Press, Cold Spring Harbor, New York.

(2) Hang, I., et al. (2015) Analysis of site-specific N-glycan remodeling in the endoplasmic reticulum and the Golgi. *Glycobiology 25*, 1335-1349.

(3) Dell, A., and Morris, H. R. (2001) Glycoprotein structure determination mass spectrometry. *Science 291*, 2351-2356.

(4) Bernardes, G. J. L., Castagner, B., and Seeberger, P. H. (2009) Combined Approaches to the Synthesis and Study of Glycoproteins. *ACS Chem. Biol. 4*, 703-713.

(5) Rich, J. R., and Withers, S. G. (2009) Emerging methods for the production of homogeneous human glycoproteins. *Nat. Chem. Biol. 5*, 206-215.

(6) Wang, L. X., and Lomino, J. V. (2012) Emerging Technologies for Making Glycan-Defined Glycoproteins. *ACS Chem. Biol. 7*, 110-122.

(7) Kiani, C., Chen, L., Wu, Y. J., Yee, A. J., and Yang, B. B. (2002) Structure and function of aggrecan. *Cell Res. 12*, 19-32.

(8) Nakato, H., and Kimata, K. (2002) Heparan sulfate fine structure and specificity of proteoglycan functions. *Biochim. Biophys. Acta, Gen. Subj. 1573*, 312-318.

(9) Dudhia, J. (2005) Aggrecan, aging and assembly in articular cartilage. *Cell. Mol. Life Sci. 62*, 2241-2256.

(10) Chabre, Y. M., and Roy, R. (2010) Design and creativity in synthesis of multivalent neoglycoconjugates. *Adv. Carbohydr. Chem. Biochem. 63*, 165-393.

(11) Kiessling, L. L., Gestwicki, J. E., and Strong, L. E. (2006) Synthetic Multivalent Ligands as Probes of Signal Transduction. *Angew. Chem., Int. Ed. 45*, 2348-2368.

(12) Renaudet, O., and Roy, R. (2013) Multivalent scaffolds in glycoscience: an overview. *Chem. Soc. Rev. 42*, 4515-4517.

(13) Hartmann, M., and Lindhorst, T. K. (2011) The Bacterial Lectin FimH, a Target for Drug Discovery–Carbohydrate Inhibitors of Type 1 Fimbriae-Mediated Bacterial Adhesion. *Eur. J. Org. Chem. 2011*, 3583-3609.

(14) Ortega-Muñoz, M., Perez-Balderas, F., Morales-Sanfrutos, J., Hernandez-Mateo, F., Isac-García, J., and Santoyo-Gonzalez, F. (2009) Click multivalent heterogeneous neoglycoconjugates–Modular synthesis and evaluation of their binding affinities. *Eur. J. Org. Chem. 2009*, 2454-2473.

(15) Lindhorst, T. K., Bruegge, K., Fuchs, A., and Sperling, O. (2010) A bivalent glycopeptide to target two putative carbohydrate binding sites on FimH. *Beilstein J. Org. Chem. 6*, 801-809.

(16) Keding, S. J., and Danishefsky, S. J. (2004) Prospects for total synthesis: a vision for a totally synthetic vaccine targeting epithelial tumors. *Proc. Natl. Acad. Sci. U.S.A. 101*, 11937-11942.

(17) Deguise, I., Lagnoux, D., and Roy, R. (2007) Synthesis of glycodendrimers containing both fucoside and galactoside residues and their binding properties to Pa-IL and PA-IIL lectins from Pseudomonas aeruginosa. *New J. Chem. 31*, 1321-1331.

(18) Gómez-García, M., Benito, J. M., Butera, A. P., Mellet, C. O., Fernández, J. M. G. a., and Blanco, J. L. J. n. (2012) Probing carbohydrate-lectin recognition in heterogeneous environments with monodisperse cyclodextrin-based glycoclusters. *J. Org. Chem. 77*, 1273-1288.

(19) Geng, J., et al. (2007) Site-directed conjugation of “clicked” glycopolymers to form glycoprotein mimics: binding to mammalian lectin and induction of immunological function. *J. Am. Chem. Soc. 129*, 15156-15163.
(20) Kikkeri, R., Laurino, P., Odedra, A., and Seeberger, P. H. (2010) Synthesis of Carbohydrate-Functionalized Quantum Dots in Microreactors. *Angew. Chem., Int. Ed. 49*, 2054-2057.
(21) Marradi, M., Chiodo, F., Garcia, I., and Penadés, S. (2013) Glyconanoparticles as multifunctional and multimodal carbohydrate systems. *Chem. Soc. Rev. 42*, 4728-4745.
(22) Slaney, A. M., et al. (2016) Conjugation of A and B Blood Group Structures to Silica Microparticles for the Detection of Antigen-Specific B Cells. *Bioconjugate Chem. 27*, 705-715.
(23) Galan, M. C., Dumy, P., and Renaudet, O. (2013) Multivalent glyco (cyclo) peptides. *Chem. Soc. Rev. 42*, 4599-4612.
(24) Gestwicki, J. E., Cairo, C. W., Borrok, M. J., and Kiessling, L. L. (2003) Visualization and characterization of receptor clusters by transmission electron microscopy. *Methods Enzymol. 362*, 301-312.
(25) Gestwicki, J. E., Cairo, C. W., Strong, L. E., Oetjen, K. A., and Kiessling, L. L. (2002) Influencing receptor-ligand binding mechanisms with multivalent ligand architecture. *J. Am. Chem. Soc. 124*, 14922-14933.
(26) Kolb, H. C., Finn, M. G., and Sharpless, K. B. (2001) Click chemistry: Diverse chemical function from a few good reactions. *Angew. Chem., Int. Ed. 40*, 2004-2021.
(27) Sletten, E. M., and Bertozzi, C. R. (2009) Bioorthogonal Chemistry: Fishing for Selectivity in a Sea of Functionality. *Angew. Chem., Int. Ed. 48*, 6974-6998.
(28) Dondoni, A., and Marra, A. (2012) Recent applications of thiol–ene coupling as a click process for glycoconjugation. *Chem. Soc. Rev. 41*, 573-586.
(29) Rostovtsev, V. V., Green, L. G., Fokin, V. V., and Sharpless, K. B. (2002) A stepwise huisgen cycloaddition process: copper (I)-catalyzed regioselective “ligation” of azides and terminal alkynes. *Angew. Chem. 114*, 2708-2711.
(30) Kottari, N., Chabre, Y. M., Shiao, T. C., Rej, R., and Roy, R. (2014) Efficient and accelerated growth of multifunctional dendrimers using orthogonal thiol–ene and SN 2 reactions. *Chem. Commun. 50*, 1983-1985.
(31) Fiore, M., Daskhan, G. C., Thomas, B., and Renaudet, O. (2014) Orthogonal dual thiol–chloroacetyl and thiol–ene couplings for the sequential one-pot assembly of heteroglycoclusters. *Beilstein J. Org. Chem. 10*, 1557-1563.
(32) Ulrich, S., Boturyn, D., Marra, A., Renaudet, O., and Dumy, P. (2014) Oxime Ligation: A Chemoselective Click-Type Reaction for Accessing Multifunctional Biomolecular Constructs. *Chem.—Eur. J. 20*, 34-41.
(33) Thomas, B., Fiore, M., Daskhan, G. C., Spinelli, N., and Renaudet, O. (2015) A multi-ligation strategy for the synthesis of heterofunctionalized glycosylated scaffolds. *Chem. Commun. 51*, 5436-5439.
(34) Sun, L., Middleton, D. R., Wantuch, P. L., Ozdilek, A., and Avci, F. Y. (2016) Carbohydrates as T-cell antigens with implications in health and disease. *Glycobiology 26*, 1029-1040.
(35) Astronomo, R. D., and Burton, D. R. (2010) Carbohydrate vaccines: developing sweet solutions to sticky situations? *Nat. Rev. Drug Discov. 9*, 308-324.

(36) Crocker, P. R., Paulson, J. C., and Varki, A. (2007) Siglecs and their roles in the immune system. *Nat. Rev. Immunol. 7*, 255-266.
(37) Meyer-Bahlburg, A., and Rawlings, D. J. (2008) B cell autonomous TLR signaling and autoimmunity. *Autoimmun. Rev. 7*, 313-316.
(38) Tsubata, T., and Wienands, J. (2001) B cell signaling. Introduction. *Int. Rev. Immunol. 20*, 675-8.
(39) Nitschke, L. (2009) CD22 and Siglec-G: B-cell inhibitory receptors with distinct functions. *Immunol. Rev. 230*, 128-143.
(40) Jellusova, J., and Nitschke, L. (2011) Regulation of B cell functions by the sialic acid-binding receptors siglec-G and CD22. *Front. Immunol. 2*, 1-14.
(41) Nitschke, L. (2014) CD22 and Siglec-G regulate inhibition of B-cell signaling by sialic acid ligand binding and control B-cell tolerance. *Glycobiology 24*, 807-817.
(42) Paulson, J. C., Macauley, M. S., and Kawasaki, N. (2012) Siglecs as sensors of self in innate and adaptive immune responses. *Annals of the New York Academy of Sciences 1253*, 37-48.
(43) Pfrengle, F., Macauley, M. S., Kawasaki, N., and Paulson, J. C. (2013) Copresentation of antigen and ligands of Siglec-G induces B cell tolerance independent of CD22. *J. Immunol. 191*, 1724-1731.
(44) Poe, J. C., and Tedder, T. F. (2012) CD22 and Siglec-G in B cell function and tolerance. *Trends Immunol. 33*, 413-420.
(45) Lanoue, A., Batista, F. D., Stewart, M., and Neuberger, M. S. (2002) Interaction of CD22 with alpha2,6-linked sialoglycoconjugates: innate recognition of self to dampen B cell autoreactivity? *Eur. J. Immunol. 32*, 348-55.
(46) Courtney, A. H., Puffer, E. B., Pontrello, J. K., Yang, Z.-Q., and Kiessling, L. L. (2009) Sialylated multivalent antigens engage CD22 in trans and inhibit B cell activation. *Proc. Natl. Acad. Sci. U.S.A. 106*, 2500-2505.
(47) Macauley, M. S., Pfrengle, F., Rademacher, C., Nycholat, C. M., Gale, A. J., von Drygalski, A., and Paulson, J. C. (2013) Antigenic liposomes displaying CD22 ligands induce antigen-specific B cell apoptosis. *J. Clin. Invest. 123*, 3074-3083.
(48) O'Reilly, M. K., Collins, B. E., Han, S., Liao, L., Rillahan, C., Kitov, P. I., Bundle, D. R., and Paulson, J. C. (2008) Bifunctional CD22 ligands use multimeric immunoglobulins as protein scaffolds in assembly of immune complexes on B cells. *J. Am. Chem. Soc. 130*, 7736-7745.
(49) Puffer, E. B., Pontrello, J. K., Hollenbeck, J. J., Kink, J. A., and Kiessling, L. L. (2007) Activating B cell signaling with defined multivalent ligands. *ACS Chem. Biol. 2*, 252-262.
(50) Shokat, K. M., and Schultz, P. G. (1991) Redirecting the immune response: ligand-mediated immunogenicity. *J. Am. Chem. Soc. 113*, 1861-1862.
(51) Rillahan, C. D., Macauley, M. S., Schwartz, E., He, Y., McBride, R., Arlian, B. M., Rangarajan, J., Fokin, V. V., and Paulson, J. C. (2014) Disubstituted sialic acid ligands targeting siglecs CD33 and CD22 associated with myeloid leukaemias and B cell lymphomas. *Chem. Sci. 5*, 2398-2406.
(52) Kawasaki, N., Rademacher, C., and Paulson, J. C. (2011) CD22 regulates adaptive and innate immune responses of B cells. *J. Innate Immun. 3*, 411-419.
(53) Abdu-Allah, H. H. M., Watanabe, K., Daikoku, S., Kanie, O., Tsubata, T., Ando, H., Ishida, H., and Kiso, M. (2011) Design and Synthesis of a Multivalent

Heterobifunctional CD22 Ligand as a Potential Immunomodulator. *Synthesis 2011*, 2968-2974.
(54) Borel, H., and Borel, Y. (1990) A novel technique to link either proteins or peptides to gammaglobulin to construct tolerogens. *J. Immunol. Methods 126*, 159-168.
(55) Mannie, M. D., and Curtis, I. I. A. D. (2013) Tolerogenic vaccines for Multiple Sclerosis. *Human Vaccines & Immunotherapeutics 9*, 1032-1038.
(56) Cockerill, K. A., Iverson, G. M., Jones, D. S., and Linnik, M. D. (2004) Therapeutic Potential of Toleragens in the Management of Antiphospholipid Syndrome. *BioDrugs 18*, 297-305.
(57) Rydberg, L. (2001) ABO-incompatibility in solid organ transplantation. *Transfusion Medicine 11*, 325-342.
(58) Fan, X., Ang, A., Pollock-BarZiv, S. M., Dipchand, A. I., Ruiz, P., Wilson, G., Platt, J. L., and West, L. J. (2004) Donor-specific B-cell tolerance after ABO-incompatible infant heart transplantation. *Nat. Med. 10*, 1227-1233.
(59) Landsteiner, K. (1900) Zur Kenntnis der antifermentativen, lytischen und agglutinierenden Wirkungen des Blutserums und der Lymphe. *Zentralblatt Bakteriologie 27*, 357-362.
(60) Franchini, M., and Liumbruno, G. M. (2013) ABO blood group: old dogma, new perspectives. *Clin. Chem. Lab. Med. 51*, 1545-1553.
(61) West, L. J., Pollock-Barziv, S. M., Dipchand, A. I., Lee, K. J., Cardella, C. J., Benson, L. N., Rebeyka, I. M., and Coles, J. G. (2001) ABO-Incompatible Heart Transplantation in Infants. *N. Engl. J. Med. 344*, 793-800.
(62) West, L. J., Karamlou, T., Dipchand, A. I., Pollock-BarZiv, S. M., Coles, J. G., and McCrindle, B. W. (2006) Impact on outcomes after listing and transplantation, of a strategy to accept ABO blood group-incompatible donor hearts for neonates and infants. *J. Thorac. Cardiovasc. Surg. 131*, 455-61.
(63) Jeyakanthan, M., Tao, K., Zuo, L., Meloncelli, P. J., Lowary, T. L., Suzuki, K., Boland, D., Larsen, I., Burch, M., et al. (2015) Chemical Basis for Qualitative and Quantitative Differences Between ABO Blood Groups and Subgroups: Implications for Organ Transplantation. *Am. J. Transplant. 15*, 2602-2615.
(64) Jeyakanthan, M., Meloncelli, P. J., Zuo, L., Lowary, T. L., Larsen, I., Maier, S., Tao, K., Rusch, J., Chinnock, R., Shaw, N., et al. (2016) ABH-Glycan Microarray Characterizes ABO Subtype Antibodies: Fine Specificity of Immune Tolerance After ABO-Incompatible Transplantation. *Am. J. Transplant. 16*, 1548-58.
(65) Cooper, D. K. C., Ye, Y., Niekrasz, M., Kehoe, M., Martin, M., Neethling, F. A., Kosanke, S., DeBault, L. E., Worsley, G., and Zuhdi, N., et al. (1993) SPECIFIC INTRAVENOUS CARBOHYDRATE THERAPY - A NEW CONCEPT IN INHIBITING ANTIBODY-MEDIATED REJECTION EXPERIENCE WITH ABO-INCOMPATIBLE CARDIAC ALLOGRAFTING IN THE BABOON. *Transplantation 56*, 769-777.
(66) Jones, D. S., Barstad, P. A., Feild, M. J., Hachmann, J. P., Hayaq, M. S., Hill, K. W., Iverson, G. M., Livingston, D. A., Palanki, M. S., and Tibbetts, A. R., et al. (1995) Immunospecific reduction of antioligonucleotide antibody-forming cells with a tetrakis-oligonucleotide conjugate (LJP 394), a therapeutic candidate for the treatment of lupus nephritis. *J. Med. Chem. 38*, 2138-44.
(67) Jones, D. S., Branks, M. J., Campbell, M. A., Cockerill, K. A., Hammaker, J, R., Kessler, C, A., Smith, E, M., Tao, A., Ton-Nu, H.-T., and Xu, T., (2003) Multivalent

poly (ethylene glycol)-containing conjugates for in vivo antibody suppression. *Bioconjugate Chem.14*, 1067-1076.

(68) Jones, D. S., Coutts, S. M., Gamino, C. A., Iverson, G. M., Linnik, M. D., Randow, M. E., Ton-Nu, H.-T., and Victoria, E. J. (1999) Multivalent Thioether− Peptide Conjugates: B Cell Tolerance of an Anti-Peptide Immune Response. *Bioconjugate Chem. 10*, 480-488.

(69) Yang, Z. Q., Puffer, E. B., Pontrello, J. K., and Kiessling, L. L. (2002) Synthesis of a multivalent display of a CD22-binding trisaccharide. *Carbohydr. Res. 337*, 1605-1613.

(70) Hossany, R. B., Johnson, M. A., Eniade, A. A., and Pinto, B. M. (2004) Synthesis and immunochemical characterization of protein conjugates of carbohydrate and carbohydrate-mimetic peptides as experimental vaccines. *Bioorg. Med. Chem. 12*, 3743-3754.

(71) Kamath, V. P., Diedrich, P., and Hindsgaul, O. (1996) Use of diethyl squarate for the coupling of oligosaccharide amines to carrier proteins and characterization of the resulting neoglycoproteins by MALDI-TOF mass spectrometry. *Glycoconj. J.13*, 315-319.

(72) Tietze, L. F., Schroeter, C., Gabius, S., Brinck, U., Goerlach-Graw, A., and Gabius, H. J. (1991) Conjugation of p-aminophenyl glycosides with squaric acid diester to a carrier protein and the use of the neoglycoprotein in the histochemical detection of lectins. *Bioconjugate Chem. 2*, 148-153.

(73) Wurm, F. R., and Klok, H.-A. (2013) Be squared: expanding the horizon of squaric acid-mediated conjugations. *Chem. Soc. Rev. 42*, 8220-8236.

(74) Zhang, J., Yergey, A., Kowalak, J., and Kovác, P. (1998) Studies towards neoglycoconjugates from the monosaccharide determinant of Vibrio cholerae O: 1, serotype Ogawa using the diethyl squarate reagent. *Carbohydr. Res. 313*, 15-20.

(75) Huang, Y.-L., Hung, J.-T., Cheung, S, K, C., Lee, H.-Y., Chu, K.-C., Li, S.-T., Lin, Y.-C., Ren, C.-T., Cheng, T.-J, R., Hsu, et al. (2013) Carbohydrate-based vaccines with a glycolipid adjuvant for breast cancer. *Proc. Natl. Acad. Sci. U.S.A. 110*, 2517-2522.

(76) Huo, C.-X., Zheng, X.-J., Xiao, A., Liu, C.-C., Sun, S., Lv, Z., and Ye, X.-S. (2015) Synthetic and immunological studies of N-acyl modified S-linked STn derivatives as anticancer vaccine candidates. *Org. Biomol. Chem. 13*, 3677-3690.

(77) Wu, X., and Bundle, D. R. (2005) Synthesis of Glycoconjugate Vaccines for Candida a lbicans Using Novel Linker Methodology. *J. Org. Chem. 70*, 7381-7388.

(78) Wu, X., Ling, C.-C., and Bundle, D. R. (2004) A new homobifunctional p-nitro phenyl ester coupling reagent for the preparation of neoglycoproteins. *Org. Lett. 6*, 4407-4410.

(79) Yu, H., Chokhawala, H. A., Varki, A., and Chen, X. (2007) Efficient chemoenzymatic synthesis of biotinylated human serum albumin–sialoglycoside conjugates containing O-acetylated sialic acids. *Org. Biomol. Chem. 5*, 2458-2463.

(80) Martin, C. E., Broecker, F., Oberli, M. A., Komor, J., Mattner, J., Anish, C., and Seeberger, P. H. (2013) Immunological evaluation of a synthetic Clostridium difficile oligosaccharide conjugate vaccine candidate and identification of a minimal epitope. *J. Am. Chem. Soc.135*, 9713-9722.

(81) Möginger, U., Resemann, A., Martin, C, E., Parameswarappa, S., Govindan, S., Wamhof, E.-C., Broecker, F., Suckau, D., Pereira, C, L., Anish, C., et al. (2016) Cross

Reactive Material 197 glycoconjugate vaccines contain privileged conjugation sites. *Scientific reports 6*, 20488.
(82) Guiard, J., Fiege, B., Kitov, P. I., Peters, T., and Bundle, D. R. (2011) "Double-Click" Protocol for Synthesis of Heterobifunctional Multivalent Ligands: Toward a Focused Library of Specific Norovirus Inhibitors. *Chem.—Eur. J. 17*, 7438-7441.
(83) Buskas, T., Li, Y., and Boons, G. J. (2004) The Immunogenicity of the Tumor-Associated Antigen Lewisy May Be Suppressed by a Bifunctional Cross-Linker Required for Coupling to a Carrier Protein. *Chem.—Eur. J. 10*, 3517-3524.
(84) Adamo, R., Nilo, A., Harfouche, C., Brogioni, B., Pecetta, S., Brogioni, G., Balducci, E., Pinto, V., Filippini, S., Morri, E., et al. (2014) Investigating the immunodominance of carbohydrate antigens in a bivalent unimolecular glycoconjugate vaccine against serogroup A and C meningococcal disease. *Glycoconj. J. 31*, 637-647.
(85) Dziadek, S., Jacques, S., and Bundle, D. R. (2008) A Novel Linker Methodology for the Synthesis of Tailored Conjugate Vaccines Composed of Complex Carbohydrate Antigens and Specific TH-Cell Peptide Epitopes. *Chem.—Eur. J. 14*, 5908-5917.
(86) Greenwald, R. B., Choe, Y. H., McGuire, J., and Conover, C. D. (2003) Effective drug delivery by PEGylated drug conjugates. *Adv. Drug Deliv. Rev. 55*, 217-250.
(87) Knop, K., Hoogenboom, R., Fischer, D., and Schubert, U. S. (2010) Poly (ethylene glycol) in drug delivery: pros and cons as well as potential alternatives. *Angew. Chem., Int. Ed. 49*, 6288-6308.
(88) Veronese, F. M., and Pasut, G. (2005) PEGylation, successful approach to drug delivery. *Drug Discov. Today 10*, 1451-1458.
(89) Zhao, H., Rubio, B., Sapra, P., Wu, D., Reddy, P., Sai, P., Martinez, A., Gao, Y., Lozanguiez, Y., Longley, C., et al. (2008) Novel prodrugs of SN38 using multiarm poly (ethylene glycol) linkers. *Bioconjugate Chem. 19*, 849-859.
(90) Meloncelli, P. J., and Lowary, T. L. (2010) Synthesis of ABO histo-blood group type I and II antigens. *Carbohydr. Res. 345*, 2305-2322.
(91) Dondoni, A. (2008) The emergence of thiol–ene coupling as a click process for materials and bioorganic chemistry. *Angew. Chem., Int. Ed. 47*, 8995-8997.
(92) Zhang, J., Zou, L., and Lowary, T. L. (2013) Synthesis of the Tolerance-Inducing Oligosaccharide Lacto-N-Fucopentaose III Bearing an Activated Linker. *ChemistryOpen 2*, 156-163.
(93) Hayashi-Takanaka, Y., Stasevich, T. J., Kurumizaka, H., Nozaki, N., and Kimura, H. (2014) Evaluation of chemical fluorescent dyes as a protein conjugation partner for live cell imaging. *PLoS One 9,* e106271.
(94) Goddard-Borger, E. D., and Stick, R. V. (2007) An efficient, inexpensive, and shelf-stable diazotransfer reagent: Imidazole-1-sulfonyl azide hydrochloride. *Org. Lett. 9*, 3797-3800.
(95) Potter, G. T., Jayson, G. C., Miller, G. J., and Gardiner, J. M. (2016) An Updated Synthesis of the Diazo-Transfer Reagent Imidazole-1-sulfonyl Azide Hydrogen Sulfate. *J. Org. Chem. 81*, 3443-3446.
(96) Carpino, L. A., and Han, G. Y. (1970) 9-Fluorenylmethoxycarbonyl function, a new base-sensitive amino-protecting group. *J. Am. Chem. Soc. 92*, 5748-5749.

(97) Dourtoglou, V., Gross, B., Lambropoulou, V., and Zioudrou, C. (1984) O-Benzotriazolyl-N,N,N′,N′-tetramethyluronium Hexafluorophosphate as Coupling Reagent for the Synthesis of Peptides of Biological Interest. *Synthesis 1984*, 572-574.
(98) Wan, Q., Chen, J., Chen, G., and Danishefsky, S. J. (2006) A potentially valuable advance in the synthesis of carbohydrate-based anticancer vaccines through extended cycloaddition chemistry. *J. Org. Chem. 71*, 8244-8249.
(99) Daskhan, G. C., Pifferi, C., and Renaudet, O. (2016) Synthesis of a New Series of Sialylated Homo- and Heterovalent Glycoclusters by using Orthogonal Ligations. *ChemistryOpen 5*, 477-484.
(100) Yu, H., Chokhawala, H. A., Huang, S., and Chen, X. (2006) One-pot three-enzyme chemoenzymatic approach to the synthesis of sialosides containing natural and non-natural functionalities. *Nat. protoc. 1*, 2485-2492.
(101) Chung, B. K., et al. (2013) Innate immune control of EBV-infected B cells by invariant natural killer T cells. *Blood 122*, 2600-2608.
(102) Imre, T., Schlosser, G., Pocsfalvi, G., Siciliano, R., Molnár-Szöllősi, É., Kremmer, T., Malorni, A., and Vékey, K. (2005) Glycosylation site analysis of human alpha-1-acid glycoprotein (AGP) by capillary liquid chromatography—electrospray mass spectrometry. *J. Mass Spectrom. 40*, 1472-1483.
(103) Razi, N., and Varki, A. (1998) Masking and unmasking of the sialic acid-binding lectin activity of CD22 (Siglec-2) on B lymphocytes. *Proc. Natl. Acad. Sci. U.S.A. 95*, 7469-7474.
(104) Courtney, A. H., Bennett, N. R., Zwick, D. B., Hudon, J., and Kiessling, L. L. (2014) Synthetic Antigens Reveal Dynamics of BCR Endocytosis during Inhibitory Signaling. *ACS Chem. Biol. 9*, 202-210.
(105) Gasparrini, F., Feest, C., Bruckbauer, A., Mattila, P. K., Müller, J., Nitschke, L., Bray, D., and Batista, F. D. (2016) Nanoscale organization and dynamics of the siglec CD22 cooperate with the cytoskeleton in restraining BCR signalling. *EMBO J. 35*, 258-280.
(106) Schneider, C. A., Rasband, W. S., and Eliceiri, K. W. (2012) NIH Image to ImageJ: 25 years of image analysis. *Nat. Methods 9*, 671-675.
(107) Kampstra, P. (2008) Beanplot: A boxplot alternative for visual comparison of distributions. *J. Stat. Softw. 28*, 1-9.

TOC GRAPHIC